Chapter 4

Depletion of the proteasome-associated deubiquitinase RPN11, but not UCHL5 and USP14, results in an extensive remodeling of the ubiquitinome.

Karen A. Sap, Karel Bezstarosti, Dick H.W. Dekkers and Jeroen A.A. Demmers

Manuscript in preparation

Abstract

The 26S proteasome is responsible for the degradation of a large complement of polyubiquitin-tagged proteins in the cell. In Drosophila melanogaster the proteasome harbors three deubiquitinating enzymes (DUBs), i.e. RPN11, UCHL5 and USP14, which are involved in the removal of ubiquitin from substrates destined for the proteasome. RPN11 is essential for the execution of protein degradation by removing the polyubiquitin tag, whereas the precise role of UCHL5 and USP14 in proteasomal degradation is still under debate. UCHL5 and USP14 have been reported to either decrease or enhance degradation of specific substrates in seemingly conflicting studies. Additionally, these DUBs have been implicated in non-proteolytic processes. All of these studies, however, monitored only one or at most a few selected proteasome substrates, or used chemical DUB inhibitors that might show off-target effects.

Here, we investigate the role of the proteasome-associated DUBs in proteasome dependent protein degradation by combining targeted dsRNA mediated knockdown of individual proteasome-bound DUBs in *Drosophila* S2 cells and large scale SILAC proteomics, ubiquitinome analysis and label free quantitative mass spectrometry. Our data imply that RPN11 is important for the structure and function of the proteasome and plays the major role in the degradation of a large majority of protein targets. In contrast, depletion of UCHL5 or USP14 or both DUBs simultaneously did not affect the structure and/or assembly of the proteasome monitored via glycerol gradient sedimentation, nor did it result in observable changes at the global proteome level. We focused specifically on the dynamics of ubiquitinated proteins upon depletion of RPN11, UCHL5 or USP14 by exploiting a diGly-peptide enrichment proteomics protocol in an attempt to identify potential targets for each of these DUBs. While many targets were identified for RPN11, virtually no specific targets for UCHL5 or USP14 were observed. Next, we tested whether a remodeling of the ubiquitinome goes together with a redistribution of the various ubiquitin pools. Overall ubiquitin levels rose over two-fold when RPN11 was depleted as compared to UCHL5 and USP14. This was in agreement with the results from the SILAC assay, where the total ubiquitin level was upregulated more than two-fold upon RPN11 depletion compared to control cells. In conclusion, even though accumulation of ubiquitin is likely to occur as a result of RPN11 depletion, an increase in the total level of ubiquitin indicates that the pool of free ubiquitin is supplemented and that ubiquitin is newly synthesized. Finally, polyubiquitin linkage type analysis did not give any indications that the three different DUBs have distinct or complementary roles with respect to linkage type cleavage specificity.

Taken together, the global proteome and ubiquitinome dynamics study presented here suggests that RPN11 serves as the major DUB in proteasomal functioning in that proteins are no longer degraded when this DUB is absent. In contrast, the roles of both UCHL5 and USP14 remain enigmatic since no major effects were observed after their depletion at the proteome level, nor at the ubiquitinome level.

Introduction

The 26S proteasome is a cellular protein complex, which plays an essential role in the degradation of proteins in the cell and, thus, in proteostasis. Proteins are typically targeted for 26S proteasome-mediated degradation through the post-translational attachment of a polyubiquitin tag (Finley, 2009). This tag is recognized by ubiquitin receptors at the proteasome 19S regulatory particle (RP), which in turn uses the tag to dock the substrate to the proteasome. Prior to proteolysis, this polyubiquitin tag has to be removed from the substrate, as this facilitates substrate translocation into the narrow pore of the 20S core particle (CP), and, additionally, allows for recycling of ubiquitin. The process of deubiquitination is carried out by specialized deubiquitinating enzymes (DUBs). In *Drosophila melanogaster*, there are three DUBs associated to the 26S proteasome: RPN11 (POH1 or PSMD14 in human), UCHL5 (also known as UCH37 or UCHL3) and USP14 (Ubp6 in *S. cerevisiae*). RPN11 and USP14 are evolutionary well conserved, whereas homologs of UCHL5 have been found in mammals and zebrafish, but not in *S. cerevisiae*. The proteasome associated DUBs RPN11, UCHL5 and USP14 belong to different deubiquitinase families, *i.e.* the JAMM, Uch and USP families, respectively (reviewed in (Komander, Clague and Urbe, 2009)). There are evident differences between these DUBs in terms of both molecular mechanism and cellular function.

RPN11 is the only essential proteasome-associated DUB (Gallery *et al.*, 2007; Finley, 2009), and is required for both the structure of the 26S proteasome and for the promotion of degradation of proteasome substrates (Maytal-Kivity *et al.*, 2002; Verma *et al.*, 2002; Yao and Robert E Cohen, 2002). Purified RPN11 is instable, but addition of RPN8 induces the formation of stable RPN8-RPN11 dimers which are catalytically active *in vitro,* albeit with a low propensity to deubiquitinate folded substrates including ubiquitin (Worden, Padovani and Martin, 2014). RPN11 and RPN8 also form heterodimers within the 26S proteasome complex where they are located at the center of the 19S Regulatory Particle (RP) (Fu *et al.*, 2002; Sanches *et al.*, 2007; Pathare *et al.*, 2014; Worden, Padovani and Martin, 2014). RPN11 is activated >100-fold when incorporated into the proteasome (Mansour *et al.*, 2015). Characteristic for RPN11 is that it removes ubiquitin chains from substrate *en bloc* by hydrolyzing the isopeptide bond between a substrate lysine and the C terminus of the first ubiquitin (Lam *et al.*, 1997; Verma *et al.*, 2002; Yao and Robert E Cohen, 2002). This activity is coupled to ATP-dependent substrate translocation into the 20S core and subsequent protein degradation (Yao and Robert E Cohen, 2002; M. J. Lee *et al.*, 2011). RPN11 acts thus relatively late in the process, that is when the proteasome is committed to degrade the substrate (Verma *et al.*, 2002). Importantly, RPN11 does not show ubiquitin linkage specificity towards di-ubiquitin substrates of different linkage types (Worden, Padovani and Martin, 2014). Taken together, co-translocational deubiquitination by RPN11 promotes substrate degradation by the 26S proteasome (Maytal-Kivity *et al.*, 2002; Verma *et al.*, 2002; Yao and Robert E Cohen, 2002; Worden, Dong and Martin, 2017).

Like RPN11, UCHL5 is a constituent subunit of the 26S proteasome in *Drosophila* (Hölzl *et al.*, 2000), mammals (Lam *et al.*, 1997) and *Schizosaccharomyces pombe* (Li *et al.*, 2000), although it seems not essential for its structure and proteolytic activity. UCHL5 is recruited to the proteasome by RPN13 and it associates with RPN2 in the 19S RP (Yao *et al.*, 2006; Chen *et al.*, 2010). The activity of UCHL5 is enhanced by RPN13 upon proteasome binding (Hamazaki *et al.*, 2006; Qiu *et al.*, 2006; Yao *et al.*, 2006). UCHL5 trims single ubiquitin moieties from the distal end of polyubiquitin chains (Lam *et al.*, 1997). In contrast, USP14 may not be a constituent subunit of the proteasome (Borodovsky *et al.*, 2001; Kuo and Goldberg, 2017), which we confirmed in this work as well (Figure 1). The amount of the USP14 homolog Ubp6 was found to be only ~30% of the canonical RP subunits in yeast as measured by quantitative label free mass spectrometry (Aufderheide *et al.*, 2015). In contrast, in HeLa cells 26S proteasomes contained approximately stoichiometric levels of USP14, but most cellular USP14 was found not to be associated with the proteasome (Elena Koulich, Xiaohua Li, 2008). The presence of ubiquitinated substrate at the proteasome promotes USP14 recruitment to the 26S proteasome (Kuo and Goldberg, 2017). USP14 interacts with proteasome subunit RPN1 via its N-terminal ubiquitin-like domain (UBL) (Elsasser *et al.*, 2002; Rosenzweig *et al.*, 2012) and its DUB activity is increased to a great extent upon binding to the 26S proteasome (Borodovsky *et al.*, 2001; David S. Leggett *et al.*, 2002; Hu *et al.*, 2005). Like for UCHL5, in the canonical model USP14 removes single ubiquitin moieties from the distal end of polyubiquitin chains (Lam *et al.*, 1997; Hanna *et al.*, 2006; M. J. Lee *et al.*, 2011), although this idea was challenged recently by Finley and coworkers, who showed that USP14 removes chains from Cyclin-B *en bloc* and showed that it can act in a very short time span even before the proteasome can initiate degradation (Lee *et al.*, 2016).

To date it is not clear how the activities of UCHL5 and USP14 affect proteasome dependent protein degradation rates or whether these DUBs might have a different substrate specificity from RPN11. Proteasomes can efficiently degrade substrates without USP14 (Hanna *et al.*, 2006; Lee *et al.*, 2010; Kim and Goldberg, 2017). In several proposed models UCHL5 and USP14 can decrease substrate degradation rates through the trimming of polyubiquitin chains from their distal ends, which results in a decreased affinity of the substrate (Lam *et al.*, 1997; Elena Koulich, Xiaohua Li, 2008; Lee *et al.*, 2010). However, UCHL5 and USP14 have also been reported to enhance degradation of substrates by the proteasome (Elena Koulich, Xiaohua Li, 2008; Mazumdar *et al.*, 2010; Mialki *et al.*, 2013). It should be noted here that such functional studies were often based on single or a limited number of substrates and many of these studies involve *in vitro* experiments with purified proteasomes. Although the differences in catalytic function between both DUBs are not clear, they have apparent redundant functions because depletion of both creates a phenotype not exhibited by depletion of either alone (Elena Koulich, Xiaohua Li, 2008). In a recent paper, Ubp6 (USP14) in yeast was shown to be activated especially when the proteasome adopts the substrate-engaged state, which suggests that its catalytic activity would

not prevent substrate degradation, but rather plays a facilitating role in substrate degradation and ubiquitin recycling (Bashore *et al.*, 2015).

Here, we investigate the roles of RPN11, UCHL5 and USP14 in proteasome-dependent protein degradation using a SILAC based proteomics approach, similarly as used in chapter 3 (Sap *et al.*, 2017). Our main objective was to monitor the dynamic behavior of the global cellular proteome and the ubiquitinome upon dsRNA mediated knockdown of the target DUBs in order to find out whether they may have a preference for specific substrates or specific polyubiquitin structures. We observed an extensive remodeling of both the proteome and the ubiquitinome upon RPN11 KD, whereas knockdown of UCHL5 KD, USP14 KD or a combination of both had virtually no effect on either the proteome or the ubiquitinome. Analysis of polyubiquitin dynamics did not reveal any specificity for linkage type for UCHL5 or USP14. Although the cellular pools of free (mono)ubiquitin and substrate conjugated (poly)ubiquitin were upregulated upon depletion of RPN11, no clear preference for any specific linkage type was observed.

We also investigated the nature of the interaction of USP14 to the proteasome in *Drosophila* by label free quantitative (LFQ) mass spectrometry. In contrast to RPN11 and UCHL5, USP14 (Ubp6) has previously been characterized as a non-constitutive interactor of the proteasome in mammals (Elena Koulich, Xiaohua Li, 2008) and yeast (David S. Leggett *et al.*, 2002; Rosenzweig *et al.*, 2012). In yeast, the Ubl domain in USP14 mediates reversible, salt-sensitive binding to the Rpn1/Rpn2 subunits (David S. Leggett *et al.*, 2002). To our knowledge, the interaction of USP14 with the proteasome has not yet been characterized in *Drosophila*. In our assays USP14 experiences salt-sensitive binding to the proteasome and therefore behaves as a weak or transient interactor, which is in agreement with its behavior in other eukaryotes.

In this study we showed that USP14 behaves like a transient interactor of the proteasome in *Drosophila*, which is in agreement with studies performed in yeast (David S. Leggett *et al.*, 2002; Rosenzweig *et al.*, 2012) and human cell lines (Elena Koulich, Xiaohua Li, 2008). Furthermore, we found that Rpn11 plays an important role in the degradation of proteolytic substrates, given its importance for proteasome complex stability, as well as its effect on both proteome and ubiquitinome dynamics upon Rpn11 KD. In contrast, the role of UCHL5 and USP14 remains elusive as we did not observe remodeling of the proteome, nor the ubiquitinome, upon depletion of UCHL5, USP14, or both of them. Furthermore, we observed a ~ 2-fold upregulation of the total pool of ubiquitin upon RPN11 KD, probably contributed via synthesis of ubiquitin, whereas we did not observe upregulation of specific polyubiquitin linkages, suggesting that the DUBs under investigation did not show a preference for specific polyubiquitin linkage types. In conclusion, our data show that RPN11 plays an important role in proteasome-mediated protein degradation, while the role of USP14 and UCHL5 is not yet clear.

Results

USP14 is a weak interactor of the proteasome complex in *Drosophila*

USP14/Ubp6 has been described as a transient or weak interactor of the proteasome in both yeast (David S. Leggett *et al.*, 2002; Rosenzweig *et al.*, 2012) and human (Elena Koulich, Xiaohua Li, 2008). Here we set out to assess the nature of the interaction of USP14 with the proteasome in *Drosophila* by specific co-immunopurification (co-IP) of the complex using antibodies against RPN8 or RPN10 followed by an LFQ proteomic approach. Negative control experiments were performed with non-specific antibodies isolated from rabbit preimmune serum (PPI). After the co-IP, protein complexes were washed using buffers containing either low, medium or high salt concentrations (50 mM, 150 mM and 500 mM KCl, respectively) to challenge the binding of the retained co-purified proteins. Weak interactors are likely to dissociate with increasing salt concentrations. IPs were performed in triplicates and purified proteins were resolved by SDS-PAGE, in-gel trypsinized and analyzed by mass spectrometry. Raw data were then analyzed using the LFQ option in the MaxQuant software suite to discriminate putative interactors from co-purifying contaminants. This strategy is based on comparing the protein abundances identified in the RPN8 or RPN10 co-IPs with those identified in the PPI (control) co-IPs, based on accumulated tryptic peptide spectral intensities. Putative interaction partners are expected to be more abundant in the RPN8 or RPN10 IPs, while, in contrast, non-specific contaminants would have an approximate 1:1 ratio as they are expected to be equally abundant in both co-IPs. Proteins present with significantly increased abundances according to two-sided T-test statistics in either of the IPs are shown in black in Figure 1. Proteasome subunits are shown in red and the three proteasomal DUBs are individually specified in the plot. USP14 was enriched to a similar extent as the other proteasome subunits below (50mM) and at physiological salt concentrations (150 mM), in both the α-RPN8 and α-RPN10 co-IPs, suggesting a stable interaction with the proteasome. In contrast, USP14 was enriched to a severely lesser extent under high salt conditions compared to other proteasome subunits. This may indicate that USP14 is a relatively weak interactor of the proteasome. This observation is in agreement with previous studies in yeast and human and may also suggest that the DUB may have additional functions in the cell as has been hypothesized before (Elena Koulich, Xiaohua Li, 2008).

RPN11 is important for the stability and activity of the 26S proteasome

To investigate the role of each of the proteasome bound DUBs we used a dsRNA mediated knockdown (KD) approach to specifically deplete for RPN11, UCHL5, USP14 or UCHL5/USP14 simultaneously (referred to here as double knockdown or '2xKD'). To test the efficiency of this approach, expression levels of target proteins were assessed by either immunoblotting (RPN11, Figure 2A) or by real time RT-qPCR (UCHL5 and USP14, Figure 2B) as no antibodies were available for the latter two. Control samples were treated with dsRNA directed against GFP, which is absent from the cells used in this study. dsRNA was added to the

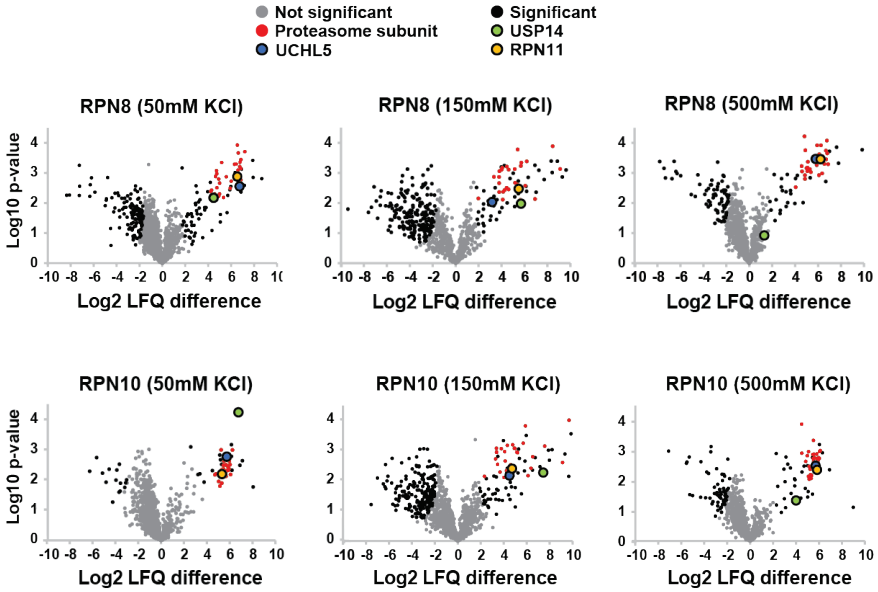

Figure 1. USP14 dissociates from the proteasome under high salt conditions in *Drosophila* S2 cells. Proteins were purified upon immunoprecipitation with antibodies directed against RPN8 or RPN10 or antibodies not specific for any proteasome subunits (Control) from whole cell extracts of S2 cells. Low, medium and high salt concentration (50 mM, 150 mM and 500 mM KCl, respectively) washing buffers were used to challenge the binding capacity of the retained purified proteins. Differential analysis of LFQ mass spectrometry results of the IPs is shown. Welch's t-tests were performed on Log2-transformed LFQ intensity values of controls (left side of volcano plots) and RPN8 or RPN10 IPs (right side). Proteins showing significantly higher abundance values are indicated in black. Proteasome subunits (red data points) were all enriched compared to control IPs, including the DUBs of interest RPN11, UCHL5 and USP14. Clearly, under increasingly stringent IP conditions, USP14 was much less effectively enriched than all other proteasome subunits, indicating a weaker binding efficiency.

cells during 48h, which is in correspondence with previous knockdown assays on different proteasome subunits (Sap *et al.*, 2017). Longer incubation times with dsRNA turned out to negatively affect cell viability. In conclusion, dsRNA mediated knockdown of RPN11, USP14 or UCHL5 results in a substantial reduction of protein expression levels (RPN11) or mRNA expression levels (UCHL5 and USP14) of the target protein products (Figures 2A and 2B), indicating that this knockdown approach is effective. dsRNA mediated interference of gene expression results in a cessation of target protein synthesis and thus also affects the assembly of novel proteasome complexes. First, we investigated the stability of the proteasome upon RPN11, USP14 or UCHL5 knockdown by glycerol gradient fractionation of protein complexes based on their size. Immunoblotting of adjacent glycerol gradient fractions shows the distribution of both

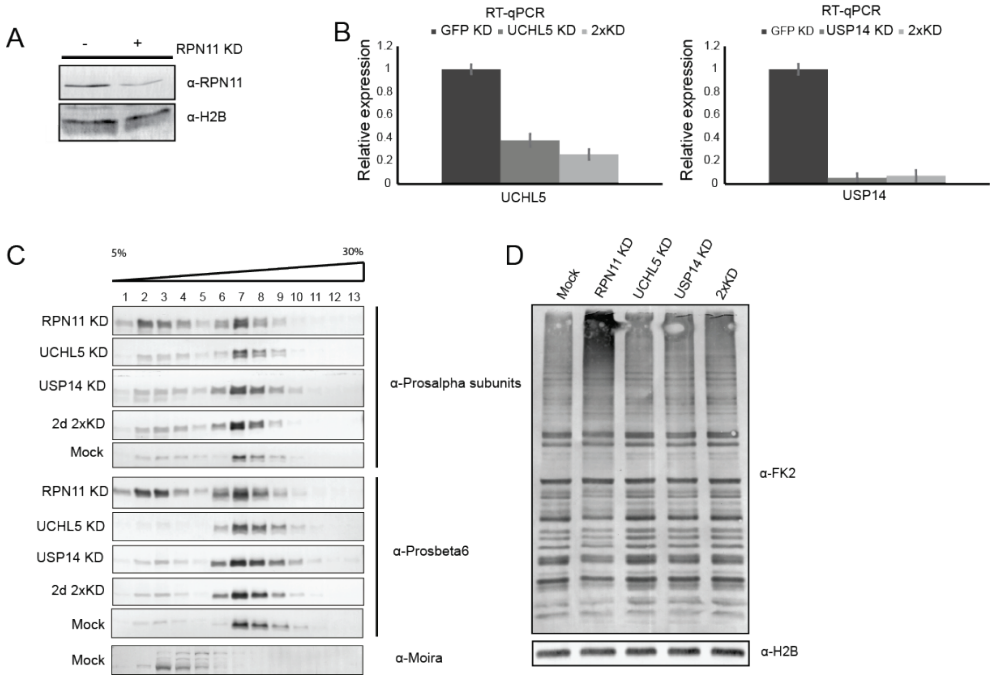

Figure 2. RPN11 is important for stability and activity of the proteasome
A) Immunoblots of RPN11 in control (left) and upon dsRNA mediated knockdown (right) in *Drosophila* S2 cells, indicating the depletion efficiency of the protocol. H2B is used as a loading control. B) UCHL5 and USP14 are downregulated upon dsRNA mediated knockdown. Since no antibodies were available for these proteins, RT-qPCR was used to assess the depletion efficiency. Total RNA was extracted from cell pellets and mRNA expression of UCHL5 and USP14 was measured (mRNA expression is shown relative to GFP dsRNA serving as the negative control here). C) Glycerol gradients were used to investigate proteasome stability upon depletion of RPN11, USP14 or UCHL5. Whole cell lysates were prepared under non-denaturing conditions and proteins and protein assemblies were separated in a 5-30% gradient. Each of the 13 resulting fractions was analyzed by SDS-PAGE and immunoblotted with α-Prosalpha and α-Prosbeta6 antibodies; α-Moira was used as a negative control. RPN11 KD affects the stability and/or assembly of the 20S proteasome core. Clearly, RPN11 knockdown results in a remarkable shift towards lower size fractions, suggesting disintegration of the 26S proteasome. D) Immunoblot with FK2 antibody of cell lysates from RPN11 KD, USP14 KD and UCHL5 KD cells. Mock cells were treated with dsRNA against GFP. RPN11 KD results in the accumulation of ubiquitinated proteins, whereas no obvious effects are observed for UCHL5 and USP14 KD.

Prosbeta6 and Prosalpha CP subunits under standard conditions (Mock, Figure 2C). As expected for intact proteasomes, distribution patterns observed for Prosbeta6 and Prosalpha subunits were comparable. The distribution patterns for Prosbeta6 and Prosalpha upon knockdown of UCHL5, USP14, and both DUBs simultaneously (2xKD) were comparable to the control

sample, whereas a substantial distribution shift to lower glycerol percentage fractions was observed upon knockdown of RPN11 (Figure 2C). This suggests that knockdown of RPN11, but not of UCHL5 and USP14, affects 26S proteasome stability to a great extent. Although the effects on proteasome stability are obvious, intact proteasomes were still observed. This may be the results of incomplete RPN11 depletion, of slow proteasome turnover or of a combination of both.

Taken together, RPN11 appears to be crucial for both proteasome stability and/or assembly, while both USP14 and UCHL5 are not. Also, the USP14/UCHL5 double knockdown did not noticeably affect proteasome stability.

Knockdown of RPN11, in contrast to UCHL5 KD, USP14 KD, or 2xKD, results in remarkable protein abundance dynamics of the global proteome

Of all proteasome associated DUBs, the role of RPN11 in promotion of protein degradation is best established (Maytal-Kivity *et al.*, 2002; Verma *et al.*, 2002; Yao and Robert E Cohen, 2002). In contrast, the roles of both UCHL5 and USP14 have not yet been fully elucidated. Several studies have shown that these DUBs can inhibit protein degradation (Lam *et al.*, 1997; Elena Koulich, Xiaohua Li, 2008; Lee *et al.*, 2010), whereas other studies have shown that they can enhance proteolysis (Elena Koulich, Xiaohua Li, 2008; Mazumdar *et al.*, 2010; Mialki *et al.*, 2013). However, in all of these studies only limited selections of specific proteasome substrates were used. We reasoned that by taking a global quantitative proteome analysis a wider range of potential substrates could be covered in order to reveal potentially specific functions for UCHL5 and USP14.

The SILAC proteomics approach in *Drosophila* S2 cells that was exploited has been described previously (Sap *et al.*, 2017). Cells were grown in culture medium with either light or heavy isotope labeled amino acids and dsRNA mediated interference of target gene expression was exploited to deplete RPN11, USP14, UCHL5 or UCHL5 and USP14 simultaneously. For control samples, dsRNA constructs to deplete for GFP were added to the cells. Label swap analyses were performed to correct for errors because of the labeling procedure. Cells were then harvested and the global proteome was analyzed by LC-MS/MS. From the heavy-to-light (H:L) ratios the relative up- or downregulation of all identified proteins as compared to the control situation could be established. The (log transformed) H:L ratio plots are shown in Figure 3. Proteins that show increased abundances because they are upregulated or accumulated as a result of the experimental condition show up in the left upper quadrant of these scatterplots. The red data points represent the knockdown target proteins in the respective assays, confirming the effectiveness of the depletion at the protein level. Proteins with either increased or decreased abundances (>1.5-fold) were considered up- or downregulated (Sap *et al.*, 2017). Only those proteins that exhibit consistent ratios in forward and reverse duplicate experiments were taken

into account for further analysis and were considered targets that specifically responded to the respective treatments.

Upon RPN11 knockdown, the global proteome is remodeled remarkably, as illustrated by the appearance of a large number of upregulated and/or accumulated proteins in the left upper quadrant. In contrast, no such an effect was observed upon knockdown of USP14, UCHL5, or the combined knockdown of these DUBs (Figure 3A). Table 1 lists the numbers of identified and quantified proteins in the various screens; Supplementary Table 1 lists all identified and quantified proteins including their H:L ratios.

Table 1. Numbers of identified and quantified proteins in global proteome datasets

Samples	Total exp #1 or #2	Total exp #1	Total exp #2	Up exp #1	Up exp #2	Up exp #1 and #2	Down exp #1	Down exp #2	Down exp #1 and #2
2d 3xKD	5381	5234	5257	810	758	535	124	146	38
RPN11 KD	5279	5085	5107	420	361	195	131	141	22
UCHL5 KD	5253	4984	5094	99	108	9	124	94	7
USP14 KD	5227	5026	4992	245	123	3	170	171	20
2d 2xKD	5293	5135	5136	117	93	5	73	117	5
4d 2xKD	4956	4711	4705	161	132	9	116	154	8

Approximately 4% of all identified proteins in the RPN11 knockdown assay were increased, while for the UCHL5 and USP14 knockdown assays only a few proteins were upregulated (Figure 3B). For reference purposes, the results of an assay in which multiple subunits (with both DUB and proteolytic activities) were knocked down simultaneously and that was published previously are included (Sap *et al.*, 2017). In this case the global proteome was remodeled extensively and approximately 10% of all detectable proteins had increased abundances.

Functional annotation analysis of increased proteins upon RPN11 knockdown revealed that many of these play a role in protein catabolic processes, cytoskeleton organization, cell cycle regulation and proteolysis (Figure 4A), which is similar to the increased protein population 3xKD (Sap *et al.*, 2017). Increased abundances of various cell cycle proteins were observed upon RPN11 knockdown (Figure 4B), which most likely are short-lived proteins that cannot be degraded anymore because of loss of proteasome functionality. Interestingly, most proteasome subunits were also increased, which is in agreement with previous reports (Wójcik and DeMartino, 2002; Lundgren *et al.*, 2005; Sap *et al.*, 2017), with the exceptions of RPT3, RPN2,

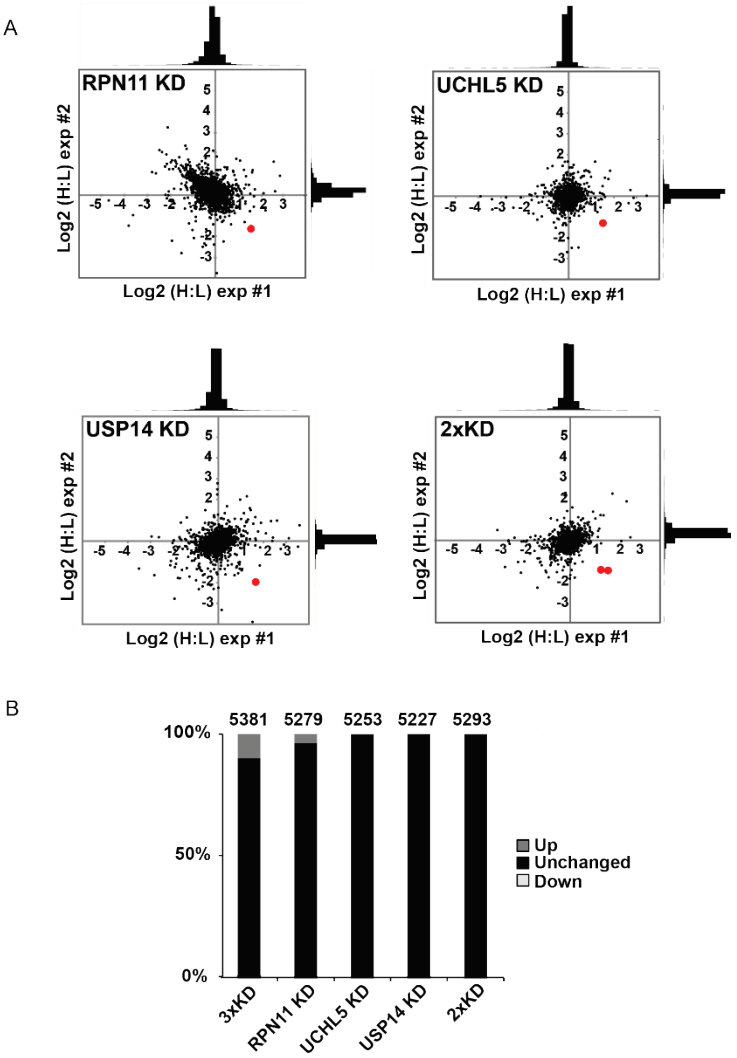

Figure 3. Depletion of RPN11, in contrast to, USP14, UCHL5 or 2xKD, results in increased abundances for a substantial part of the global proteome. A) Scatterplots of normalized forward and reverse SILAC ratios for cells in which DUBs have been knocked down versus control cells. Proteins with increased abundances appear in the left upper quadrant, proteins with decreased abundance in the right lower quadrant. The red data points indicated the proteins targeted for knockdown in the respective assays. B) The percentage of identified proteins whose abundances are affected in the global proteome dynamics assay. Approximately 4% of the global proteome was increased upon RPN11 KD. For comparative purposes, the abundance changes as a result of complete proteasome activity abolishment upon simultaneous dsRNA mediated knockdown of Prosalpha5, Prosbeta6 and RPN11 (referred to as '3xKD' and published previously (Sap *et al.*, 2017) is shown (approximately 10% of the global proteome).

RPN6, and RPN10 (Figure 4C). The reason for the aberrant behavior of these four subunits is unclear and needs to be investigated further. Possibly, these specific subunits have different turnover characteristics because of extraproteasomal functions, several of which have been described in the literature (*e.g.* for RPN10 (Matiuhin *et al.*, 2008)) or because of their specific role in the assembly of the 26S proteasome (reviewed in (Hochstrasser, 2013)). In accordance with a model where protein degradation is inhibited as a result of RPN11 lacking proteasomes and proteins are likely to be accumulated, there are only very few proteins quantified with decreased abundances upon RPN11 KD (Table S1). These proteins are most likely expressed to a lesser extent as a result of the stress induced upon the system. In contrast to the RPN11 knockdown, the effects as a result of the UCHL5, USP14 or combined knockdown were much less severe. The levels of only very few proteins were either increased or decreased in these experiments (Table S2, S3).

We have previously observed that several proteins are upregulated at a fast rate as a result of the stress imposed on the cell by inactivating the proteasome, most notably several stress response proteins, such as heat shock proteins (Sap *et al.*, 2017). Although it is not possible to differentiate between protein biosynthesis and accumulation based on these SILAC assays alone, we can assume based on these earlier studies that heat shock proteins in the RPN11 KD that are increased are also synthesized as a response to the knockdown. There is no indication that a similar response takes place in cells lacking USP14 or UCHL5. It is obvious that only in the RPN11 KD the global proteome was remodeled to some extent, while in the other cases protein abundances remained largely unchanged. There is a substantial overlap in increased proteins upon 3xKD (Sap *et al.*, 2017) and RPN11 KD: 75% of the increased proteins in RPN11 KD were also more abundant upon 3xKD (Figure 4D).

Based on these results we argue that knockdown of RPN11 alone has essentially a similar effect on global proteome dynamics as abolishing both DUB activity (by depletion of RPN11) and proteolytic activity (by depletion of Proasalpha5 and Prosbeta6) simultaneously. Altogether, these data confirm that RPN11 is essential for proper functioning of proteasome-mediated protein degradation. In contrast, while RPN11 promotes protein degradation, both UCHL5 and USP14 do not noticeably enhance nor inhibit proteasome-mediated protein degradation, at least as assessed by accumulation of proteins in a proteome-wide SILAC screen.

In conclusion, although for the RPN11 knockdown an increased remodeling of the global proteome was observed, we did not observe a major impact on global proteome dynamics upon depletion of UCHL5, USP14 or both enzymes simultaneously, suggesting that these DUBs do not seem to play a general role in the degradation of a major complement of cellular proteins.

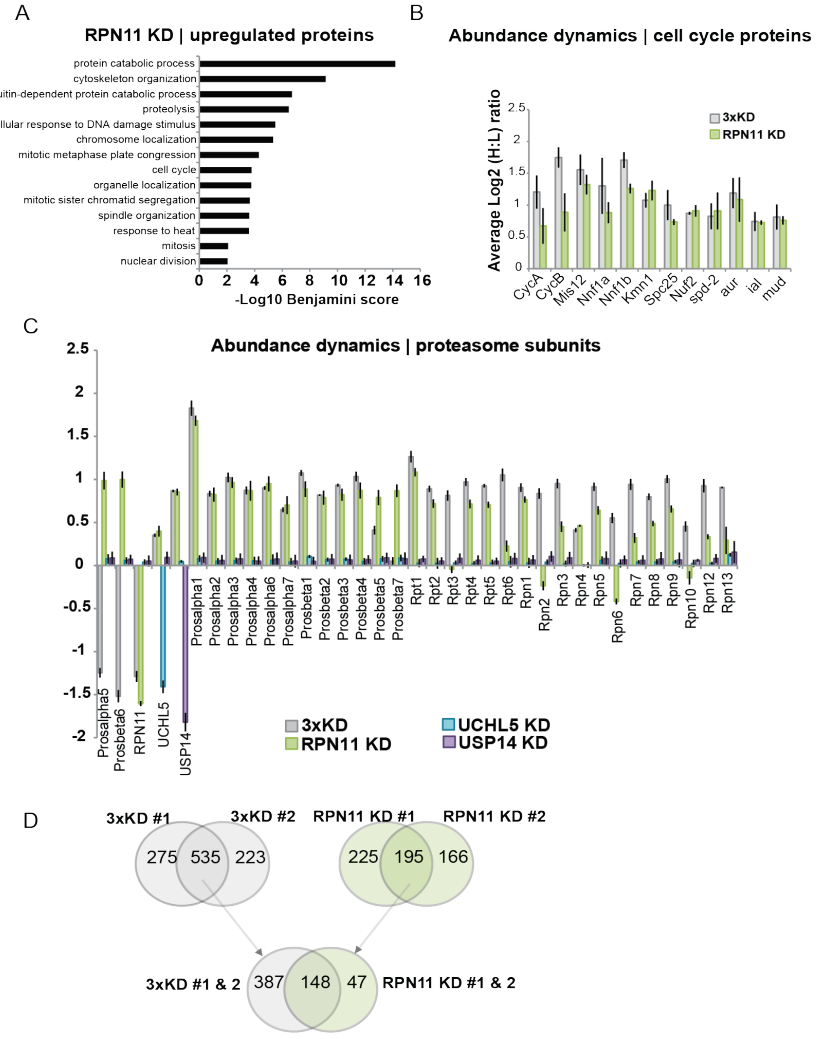

Figure 4. Cell cycle, mitotic spindle and UPS regulators are increased upon RPN11 depletion. A) Gene Ontology (GO) analysis of proteins with increased abundance upon RPN11 depletion. Functional annotation analysis was performed and a representative selection of enriched biological process GO terms is shown (enrichment probability represented by –Log10 Benjamini score). B) Abundance increases of a selection of proteins involved in cell cycle regulation and mitotic spindle organization. C) Average normalized SILAC ratios of all subunits of the proteasome show that all proteasome components, except RPT3, RPN2, RPN6 and RPN10, are upregulated or accumulated upon depletion of RPN11, but not of USP14 or UCHL5. '3xKD' represents the simultaneous knockdown of Prosalpha5, Prosbeta6 and RPN11 (Sap *et al.*, 2017) and functions as a reference dataset in this study. D) Overlap of proteins with increased

abundance upon RPN11 KD and complete proteasome activity abolishment showing that ~75% of all proteins present with increased abundance upon RPN11 KD was also more abundant upon 3xKD.

Knockdown of RPN11, in contrast to UCHL5 and USP14, results in extensive ubiquitinome remodeling

One reason could be that the mode of action and specificity of these DUBs, in contrast to RPN11, cannot be assessed by monitoring the global proteome dynamics alone. We hypothesized that UCHL5 and USP14 may have specific functions which do not *per se* result into changing protein abundances. We therefore decided to further focus on the effects of the target ubiquitination process itself by monitoring both the global ubiquitin levels as well as the dynamic 'ubiquitinome'. The rationale here is that proteins with increased ubiquitination upon knockdown of a DUB are likely to be substrates for that specific DUB.

Proteins targeted for proteasome dependent degradation are generally tagged with (poly-)ubiquitin chains. Therefore, a quantitative determination of ubiquitinated proteins may serve as a tool to monitor proper proteasome functioning in the cell. First, we assessed global levels of ubiquitin in cells lacking RPN11, USP14 or UCHL5 using western blots and detection by an FK2 antibody, which recognizes only conjugated ubiquitin. A detectable increase in the level of protein ubiquitination could only be observed upon RPN11 KD (Figure 2D). In cells under USP14 or UCHL5 knockdown conditions no changes in ubiquitination levels were observed.

Next, we tested whether a remodeling of the ubiquitinome goes together with a redistribution of the various ubiquitin pools (*i.e.*, free, monomeric and polymeric conjugated, activated) and whether changes in the total amount of free mono-ubiquitin occur. The free ubiquitin pool has been suggested to be a rate limiting factor in the ubiquitination process (Hanna, Leggett and Finley, 2003) and the amount of free monomeric ubiquitin in relation conjugated and polyubiquitin highly depends on the cell type (Kaiser *et al.*, 2011). We used protein separation by SDS-PAGE combined with label free quantitation by mass spectrometry (Figure 5A) and found that the amount of free ubiquitin in the RPN11 KD is twice as high as in the 2xKD (Figure 5B). The level of poly- and/or conjugated (poly)ubiquitin was about three times higher than that of free ubiquitin, both for the RPN11 KD as for the 2xKD samples (figure 5B). This means that overall the ubiquitin levels become approximately twice as high when RPN11 is depleted as compared to the depletion of UCHL5 and USP14. This is in agreement with the results from the SILAC assay, where the total ubiquitin level (*i.e.*, the sum of free, mono-, conjugated and polyubiquitin) was upregulated almost 2-fold (Figure 5C).

In conclusion, even though accumulation of ubiquitin is likely to occur as a result of RPN11 depletion, an increase in the total level of ubiquitin suggests that the pool of free ubiquitin is supplemented and that ubiquitin is newly synthesized

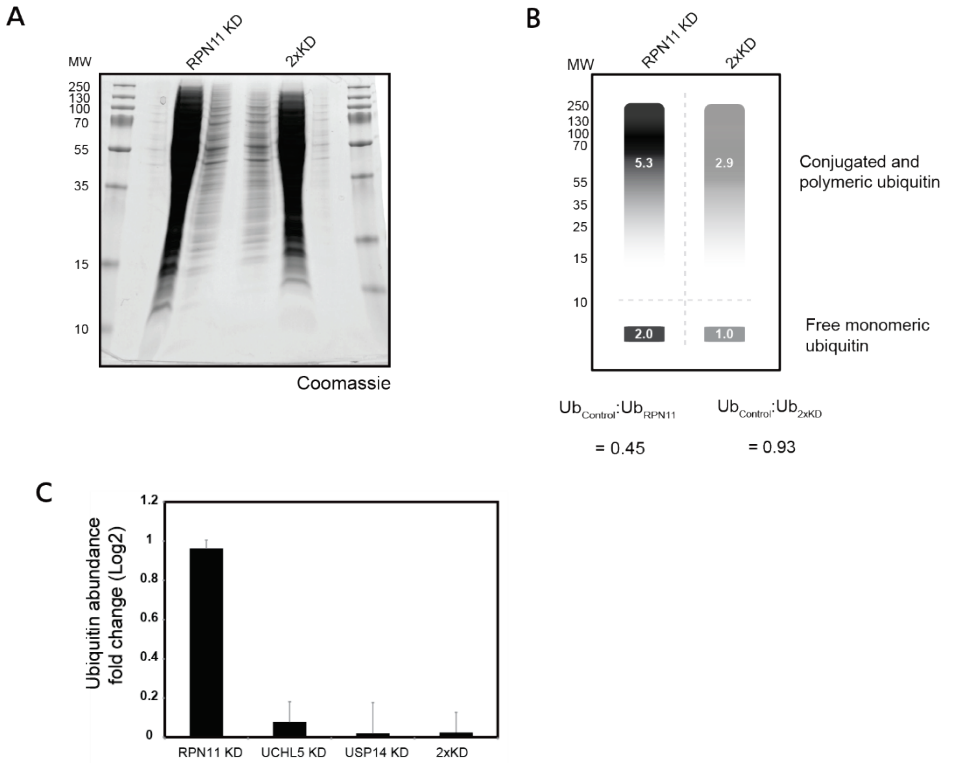

Figure 5. Upregulation of the monomeric free and polymeric and conjugated ubiquitin pools upon RPN11 KD. A) *Drosophila* S2 cells were treated for 2 days with dsRNA against RPN11 or against UCHL5 and USP14. Lysates were resolved by SDS-PAGE and Coomassie stained. Both lanes were subjected to LFQ-based mass spectrometry. B) Quantification of the free monomeric ubiquitin pool (< 10kDa) and the conjugated and polymeric ubiquitin pool (>10kDa) upon RPN11KD and 2xKD by LFQ based LC-MS/MS of samples shown in 5A. The amount of free ubiquitin in the RPN11 KD is twice as high as in the 2xKD. C) Quantification of the abundance dynamics of the total pool of ubiquitin in the global proteome datasets. ~ 2-fold upregulation of the total pool of ubiquitin upon RPN11 KD.

Next, we applied a strategy where we used monoclonal antibodies to enrich for peptides derived from ubiquitinated proteins after trypsin digestion ('diGly' peptides) to monitor the dynamics of the ubiquitinome, the complement of all ubiquitinated proteins in a cell (Kim, Eric J. Bennett, *et al.*, 2011; Wagner *et al.*, 2011; Udeshi *et al.*, 2012; Sap *et al.*, 2017). We have previously applied this technology to study the ubiquitinome in cells that completely lack proteasomal activity. Here, we combine SILAC proteomics, dsRNA mediated knockdown of RPN11, UCHL5 and USP14 with the analysis of the ubiquitinome to investigate the functional roles of these DUBs. Upon RPN11 KD, the majority of diGly peptides were upregulated as compared to the control

situation, suggesting an increase in the extent of ubiquitination for many proteins and, therefore, extensive remodeling of the ubiquitinome (Figure 6A). It should be noted here that the new ubiquitination events, in which cases peptides in the control situation would not carry a diGly remnant at all, are not included in this plot by definition. All diGly peptides, including those with no corresponding detection in the control, are listed in Supplementary Table 2 with their H:L ratios.

Table 2 lists the numbers of identified and quantified diGly peptides for each dataset, where 1.5-fold changes were used as threshold values for either up- or downregulation. Only peptides identified and quantified in both forward and reverse SILAC experiments and with consistent ratios were taken into account for further analysis. Upon RPN11 KD, more than 70% of all diGly peptides were upregulated. Functional annotation analysis revealed that the proteins they are associated with play diverse roles in the cell, such as protein catabolic processes, the cell cycle and programmed cell death (Figure 6B). Several proteins with downregulated ubiquitination sites were identified (Table S4), including ribosomal and transport proteins.

Table 2. Numbers of identified and quantified diGly modified peptides

Samples	Total	Total FW	Total REV	Up FW	Up REV	Up FW & REV	Down FW	Down REV	Down FW & REV
2d 3xKD	8211	7780	2956	6716	2173	1756	278	182	82
Rpn11 KD	4210	3427	2752	2355	1873	1089	148	97	36
UCHL5 KD	1758	1442	1226	107	54	3	33	55	8
USP14 KD	2860	2098	2406	280	89	2	167	298	11
2d 2xKD	4009	3674	2651	215	119	2	153	156	0
4d 2xKD	3526	2701	3209	172	173	12	98	202	0

In sharp contrast, the abundances of only a very small set of diGly peptides were affected upon knockdown of both UCHL5 and USP14 whereas those of the majority remained unchanged (Table 2, Table S5). Of the few cases where the extent of ubiquitination is affected, ribosomal proteins (in the UCHL5 knockdown) and ATP synthesis proteins (in the USP14 knockdown) were remarkable. Downregulated diGly peptides upon USP14, UCHL5 or 2d 2xKD were all associated with ribosomal proteins (Table S6).

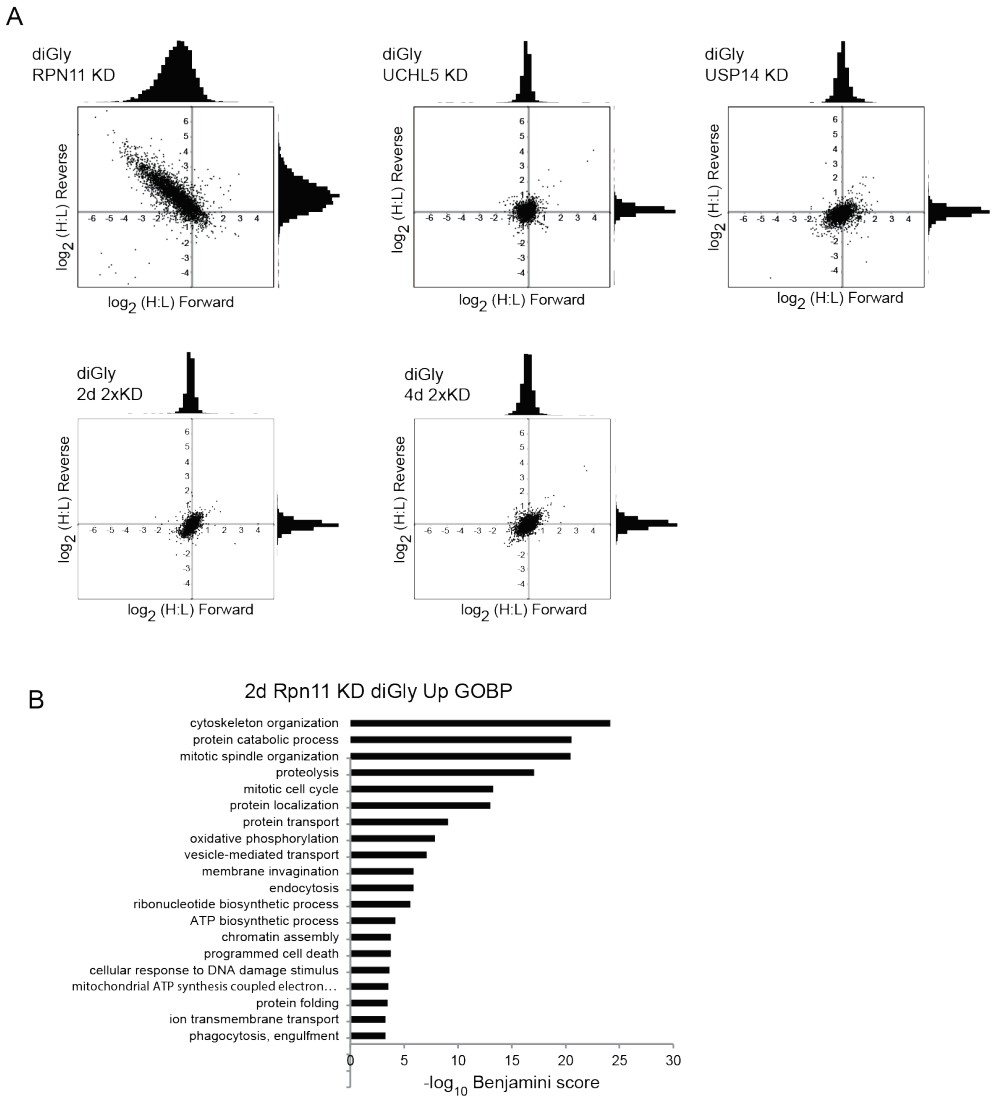

Figure 6 | Remodeling of the global ubiquitinome as a result of proteasome associated DUB interference. A) Abundance increases of diGly peptides derived from proteins in cells upon depletion of the indicated DUB. Data are from duplicate SILAC (forward and reverse) experiments. B) GO analysis of proteins with associated upregulated diGly peptides; a representative selection of enriched biological process terms is shown (enrichment probability represented by –Log10 Benjamini score).

Proteasomes contain at least three DUBs that remove ubiquitin chains from substrates. It has been hypothesized that their intrinsic linkage preference might therefore affect the residence time of a substrate at the proteasome lid (Finley, 2009). Thus, it could be that, although UCHL5 and USP14 do not seem to target specific proteins, their suggested polyubiquitin chain editing function could have an effect on the relative amounts of specific linkage types. In order to investigate whether this may be true for the proteasome-associated DUBs under investigation in this study we decided to focus on polyubiquitin derived diGly peptides. In the RPN11 KD assay, all polyubiquitin specific diGly peptides and non-modified peptides were upregulated (Figure 7A). This is in agreement with earlier findings that the relative abundances of ubiquitin increase as an effect of destabilizing this DUB. Although most diGly peptides are upregulated 1.4 – 2.3 fold, the diGly peptide representing the K27 linkage stands out at >5-fold upregulation (Figure 7A). This is unexpected, since the canonical linkage type for proteasome mediated degradation is K48 and would therefore be expected to become accumulated in the absence of proteasome DUB activity.

In contrast, for the USP14 KD, UCHL5 KD and the double knockdown (2xKD), diGly peptides did not show significant up- or downregulation and no preference or specificity for any of the polyubiquitin linkage types was observed. These data do therefore not give conclusive information on the putative editing function of both UCHL5 and USP14 (Figure 7A, 7B).

In conclusion, major changes in diGly peptide abundances were observed upon RPN11 KD, suggesting that an extensive remodeling of the ubiquitinome takes place upon depletion of RPN11. The affected diGly peptide population shows a remarkable overlap with the ubiquitination sites observed after complete abolishment of the proteasome (Sap *et al.*, 2017), indicating that either the catalytic activity and/or the structural role of RPN11 within the proteasome is important for proteasome-dependent protein degradation. In contrast, depletion of UCHL5, USP14 or both enzymes simultaneously did not lead to detectable modulation of the ubiquitinome. This observation suggests that either these DUBs do not target a broad range of protein substrates for deubiquitination or that the sensitivity of the assay is a limiting factor. Also, no specificity for specific polyubiquitin linkage types could be detected for USP14 and UCHL5. For RPN11, K27 linked polyubiquitin seems to be upregulated and/or accumulated to a higher extent than other linkage types. Taken together, our data show that knockdown of RPN11 results in a substantial increase of both protein abundance and protein ubiquitination, suggesting inhibition of proteasome-dependent degradation of a large complement of proteins in *Drosophila* S2 cells. On the other hand, knockdown of two other proteasome-associated DUBs, UCHL5 and USP14, did not result in detectable changes in the proteome, the ubiquitinome nor in the linkage-type specific composition of polyubiquitin.

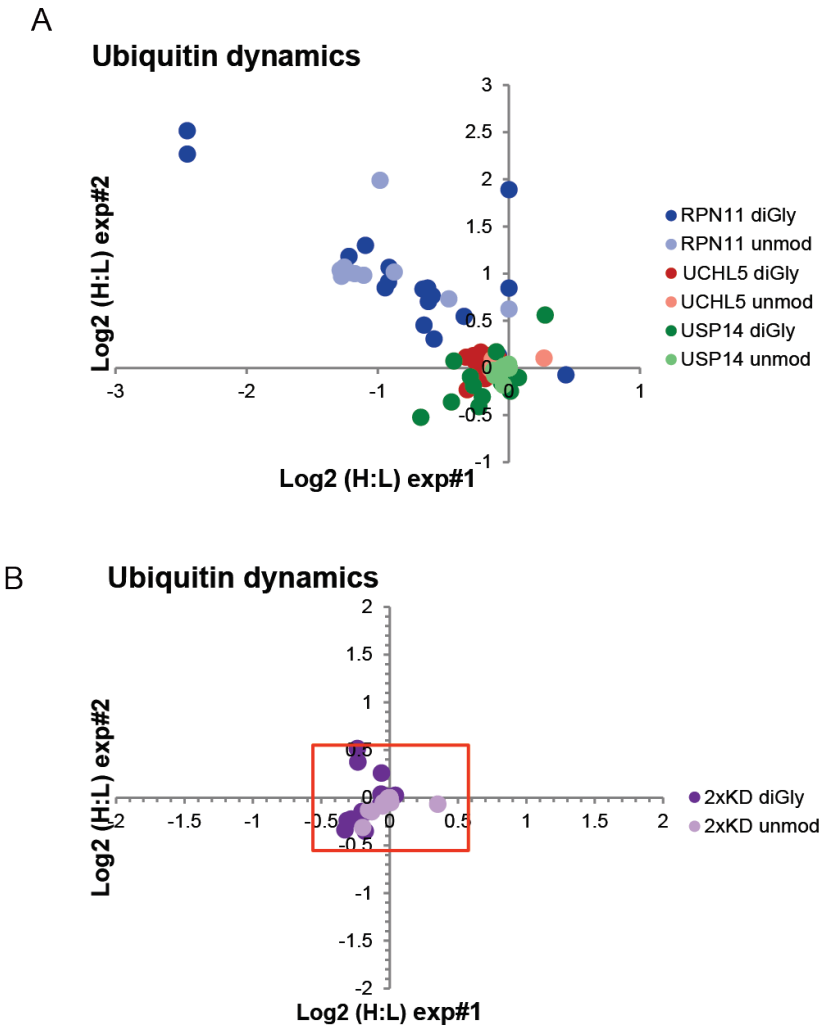

Figure 7. Ubiquitin linkage dynamics upon proteasome-bound DUB knockdown
A) Log2 fold changes of both unmodified and diGly-modified ubiquitin peptides upon single DUB knockdown of RPN11, UCHL5 or USP14. Fold changes of both modified and unmodified ubiquitin peptides were unaffected upon KD of UCHL5 or USP14. Fold changes of both modified and unmodified ubiquitin peptides upon RPN11 KD were increased about 1.4 – 2.3 fold, suggesting that the total pool of ubiquitin was upregulated including the conjugated ubiquitin pool. The top left corner shows two strongly upregulated ubiquitin K27 diGly-modified ubiquitin peptides. B) Fold changes of both modified and unmodified ubiquitin peptides were not affected upon simultaneous KD of both UCHL5 and USP14. Red box shows 1.5-fold upregulation cutoff.

Discussion

In this study, we set out by assessing the stability of three DUBs that have been extensively reported as being constituent subunits of the proteasome. For this purpose, proteasomes were isolated from *Drosophila* S2 cells by immunoprecipitation of Rpn8 or Rpn10 and washed under increasingly stringent buffer conditions. Label free quantitative mass spectrometry revealed that the strength of interaction of RPN11 and UCHL5 with the proteasome was comparable with other proteasome subunits, whereas the interaction of USP14 with the proteasome was completely lost at high salt concentrations. This result indicates USP14, but not RPN11 and UCHL5, is a relatively weak or transient interactor of the proteasome and suggests that it is not a constitutive subunit.

Next, we have investigated the effect of depletion of three known proteasome-associated DUBs by dsRNA-mediated knockdown on the UPS by monitoring both the global proteome and ubiquitinome dynamics in *Drosophila* S2 cells. While the global proteome and especially the ubiquitinome were extensively remodeled upon depletion of RPN11, the effects at the global proteome and ubiquitinome level were surprisingly small or simply absent upon depletion of USP14 or UCHL5. These findings indicate that RPN11 deubiquitinase activity plays an important role in proteasome-mediated protein degradation whereas the roles of UCHL5 and USP14 in general proteostasis remain unclear. Furthermore, we found that RPN11, but not USP14 or UCHL5, is essential for the assembly and/or stability of the proteasome. Therefore, the possibility that the absence of a stable proteome holocomplex and not the absence of deubiquitinase activity alone is responsible for the observed effects cannot be excluded. Interestingly, USP14, in contrast to RPN11 and UCHL5, was found to interact with the proteasome in a reversible manner. This suggests that it could have an additional cellular role apart from its deubiquitinase activity as part of the proteasome.

Some of our findings confirm previously reported observations in the literature. The importance of RPN11 for both the stability and the activity of the proteasome has been reported in various studies (Maytal-Kivity *et al.*, 2002; Yao and Robert E Cohen, 2002; Gallery *et al.*, 2007; Elena Koulich, Xiaohua Li, 2008; Finley, 2009). As a consequence, it is not straightforward to design assays to characterize the biological function of this subunit. Several studies have attempted to functionally characterize RPN11 by using active site mutants in yeast, *Drosophila* or human cell lines. Although one such study in yeast indeed described a viable RPN11 site-mutant (Guterman and Glickman, 2004), in all other studies these mutants were non-viable (unpublished data from our lab, Verma *et al.*, 2002; Yao and Robert E Cohen, 2002; Lundgren *et al.*, 2003; Gallery *et al.*, 2007). These findings underline its relevance also in a cellular context. Our finding that depletion of UCHL5 does not affect the stability and - seemingly - the activity of the proteasome is in agreement with reported data showing that RNAi of UCHL5 in *Drosophila* S2 cells had little apparent effect on the structure or peptidase activities of the 26S proteasome (Wójcik and

DeMartino, 2002). Additionally, no increase in the level of ubiquitinated proteins was observed. Furthermore, it has been shown that USP14 dissociates from the proteasome upon increased salt concentrations, whereas there was only little effect on UCHL5 or RPN11 under the same conditions, which is in agreement with our data (Elena Koulich, Xiaohua Li, 2008). Recently it was shown that USP14 cycles towards the proteasome upon the presence of ubiquitinated substrates at the proteasome complex and after degradation of the substrate, USP14 subsequently dissociates from the proteasome (Kuo and Goldberg, 2017).

Our results do not confirm the model that describes UCHL5 and USP14 as DUBs that antagonize substrate degradation (Lam *et al.*, 1997; Elena Koulich, Xiaohua Li, 2008; Lee *et al.*, 2010). In this model, UCHL5 and USP14 initiate the removal of ubiquitin from substrates upon docking of the ubiquitinated substrate at the proteasome ubiquitin receptors, whereby they trim polyubiquitin chains from the distal end (Lam *et al.*, 1997; Hu *et al.*, 2005; M. J. Lee *et al.*, 2011). The shortening of polyubiquitin chains may then result in a decreased binding capacity of substrate to the proteasome which in turn could slow down degradation rates or even prevent the degradation of substrate. Cohen and coworkers observed enhanced degradation of especially monoubiquitinated globin peptides and other lower–order conjugates upon isopeptidase inhibition by Ub-aldehyde *in vitro* (Lam *et al.*, 1997). Their results suggest that an 'editing isopeptidease' could decrease the degradation rates of substrates which are poorly ubiquitinated. Finley and coworkers have shown that inhibition of USP14 by the small molecule inhibitor IU1 enhances the degradation of Cyclin B and of Sic1 *in vitro* (Lee *et al.*, 2010). They hypothesized that deubiquitination of substrates by USP14 at a faster rate than the proteasome initiates degradation could cause rejection of otherwise competent substrates from the proteasome. In addition, they observed reduced levels of tau, TDP-43 and ataxin-3 upon IU1 treatment in murine embryonic fibroblasts, although others were unable to confirm a robust role for USP14 in tau or TDP-43 degradation (Ortuno, Carlisle and Miller, 2016). DeMartino and coworkers showed reduced levels of ubiquitinated proteins upon RNAi mediated knockdown of USP14 or UCHL5 in HeLa cells, although a double knockdown of UCHL5 and USP14 counteracted this effect (Elena Koulich, Xiaohua Li, 2008). b-AP15, a chemical inhibitor of both UCHL5 and USP14, has been shown to elicit a similar response as the proteasome inhibitor Bortezomib, which results in an accumulation of ubiquitinated proteins (D'Arcy *et al.*, 2011; Brnjic *et al.*, 2013; Feng *et al.*, 2014; Tian *et al.*, 2014; Wang *et al.*, 2014). However, the specificity of this small molecule drug is contested by others and unspecific inhibition of other proteasome subunits may occur, thereby blurring the effects of UCHL5 and USP14 (Huang, Jung and Chen, 2014).

The canonical signal for proteasome-dependent degradation is the presence of K48-linked polyubiquitin chains on substrate. An editing function for USP14 or UCHL5 would result in an upregulation of K48-polyubiquitin linkages upon knockdown of the respective DUBs. An *in vitro* study using di-ubiquitin probes revealed that USP14 had a preference for K11, K33 and K48 linkages (Flierman *et al.*, 2016). We did not observe an upregulation of polyubiquitin linkages,

neither did we observe an upregulation in total ubiquitin levels upon KD of USP14, UCHL5, or both of them. Altogether, we cannot confirm these studies in that we did not observe major protein abundance dynamics upon knockdown of USP14 and/or UCHL5 at a proteome-wide scale. *Drosophila* homologs of tau, TDP-43 and ataxin-3 were not identified in this study. We also did not observe abundance dynamics of ubiquitin and polyubiquitin linkages.

In contrast to the editing model, recent data from Finley and coworkers suggests that USP14 removes ubiquitin chains *en bloc* and very fast, *i.e.* before the proteasome can initiate degradation (Lee *et al.*, 2016). *In vitro* experiments with Cyclin-B, the canonical substrate of USP14, showed that all supernumery chains were removed until a single ubiquitin chain remained. In our study, we did not observe a change in abundance at the global proteome level upon USP14 knockdown, although this finding is not in disagreement with those *per se*. No diGly peptides were identified for Cyclin-B and, thus, no information is available on the extent of Cyclin-B ubiquitination as an effect of USP14 depletion.

The findings of our study are not in disagreement with a model in which USP14 (Ubp6) is a DUB that can facilitate substrate degradation by non-catalytically delaying the degradation process in order to provide a time window to allow gradual deubiquitination of the substrate. In this model, ubiquitin-bound USP14 interferes with degradation-coupled RPN11-mediated *en bloc* deubiquitination of polyubiquitin chains (Hanna *et al.*, 2006; Peth, Besche and Goldberg, 2009; Aufderheide *et al.*, 2015; Bashore *et al.*, 2015). Furthermore, ubiquitin-bound USP14 causes the proteasome to adopt the substrate-engaged conformational state, which is characterized by the coaxial alignment of the regulatory particle base subunits and the channel of the 20S core particle, and this state positions RPN11 close to the entrance of this channel (Matyskiela, Lander and Martin, 2013; Unverdorben *et al.*, 2014). Proteasomes which adopt the substrate-engaged state cannot process new substrates (Bashore *et al.*, 2015). Both mechanisms, locking the proteasome in the substrate-engaged state and inhibiting the deubiquitinating activity of RPN11, are mechanisms by which USP14 can delay substrate degradation (Aufderheide *et al.*, 2015; Bashore *et al.*, 2015). This would suggest USP14 acting as a timer to coordinate individual substrate processing steps at the proteasome, thereby facilitating, but not regulating, protein degradation. These mechanisms do not require the catalytic activity of USP14, but merely require its ability to bind ubiquitin. The catalytic activity of USP14, on the other hand, plays a role in ubiquitin recycling and is important for the maintenance of the free ubiquitin pool. It should be noted though that this model was proposed based on experiments in *S. cerevisiae*, which lacks (an ortholog of) UCHL5. Therefore, it may not be directly translated to higher eukaryotes that express both UCHL5 and USP14.

The reason that we did not observe major changes at the global proteome level upon depletion of USP14 in our assay may be explained by the property of USP14 to only temporarily delay substrate degradation for correct processing of the ubiquitin-substrate conjugate.

Several studies have shown that ubiquitin undergoes accelerated degradation by the proteasome in the absence of USP14/Ubp6 *in vivo* (David S. Leggett *et al.*, 2002; Chernova *et al.*, 2003; Hanna, Leggett and Finley, 2003; Hanna *et al.*, 2006). We did not observe a depletion of total ubiquitin upon simultaneous depletion of USP14, UCHL5 or both DUBs simultaneously (2xKD). In contrast, ubiquitin was upregulated upon RPN11 depletion. Our assay did not allow comparing differences between free ubiquitin levels in USP14 depleted cells versus control cells. Ubiquitin levels are highly regulated in the cell and an elaborate evaluation of the effects of UCHL5 and USP14 depletion on the total ubiquitin pool, the free ubiquitin pool, but also on the proteasome-bound ubiquitin pool would be an interesting supplement for this study.

Although the 26S proteasome contains approximately stoichiometric levels of UCHL5 and USP14 (Figure 1B) (Elena Koulich, Xiaohua Li, 2008), both DUBs also have a substantial non-proteasomal population, which could serve as a latent protein reservoir or may have other functions related or unrelated to their catalytic activity. *In vitro* studies have shown that RPN11 (Mansour *et al.*, 2015), UCHL5 (Yao *et al.*, 2006) and USP14 (David S. Leggett *et al.*, 2002; Hu *et al.*, 2005; Hanna *et al.*, 2006; Lee *et al.*, 2010; Bashore *et al.*, 2015) have relatively low activity outside the proteasome holocomplex. We cannot rule out the possibility that the approximately three-fold depletion of UCHL5 and USP14 levels by dsRNA mediated knockdown in our assay may be – partially or exclusively - targeted at the free, non-proteasomal protein population. In that case, large effects would not be observed because of the supposed relative low DUB activity of these proteins when not associated to the proteasome. On the other hand, the results of the RPN11 knockdown assay have shown that even a three-to-four-fold depletion is sufficient to detect major differences.

Perspective

One possibility is that the sensitivity of our assay is not sufficiently high to pick up a potentially highly specific, but only small set of target proteins. We are currently improving the coverage and sensitivity of the diGly IP assay (Van Der Wal *et al.*, 2018). Another possibility may be that the knock-down efficiency is too low and that the remaining population of the target DUB may prevent clear effects in the assay. One solution for this is to create knock-out cell lines, although it remains to be seen whether these would be viable. Finally, it cannot be excluded that the activities of UCHL5 and USP14 are indeed affected in the knockdown albeit in such a way that the readout that we have used here is inadequate to measure these effects. For instance, clipping off a single ubiquitin subunit from the distal end of a polyubiquitin chain for editing purposes may not noticeably affect the degradation rate of the target, nor may it affect the redistribution of ubiquitin pools if the removed ubiquitin residue would somehow not be included in the pool of monomeric free ubiquitin. In both the dynamic global proteome and ubiquitinome assays described here such events would go unnoticed.

Material and Methods

Nomenclature for the 26S proteasome: the core 20S proteasome subunits are designated by the α/β nomenclature and the 19S subunits are designated by the Rpn/Rpt nomenclature (Finley *et al.*, 1998).

Cell culture: *Drosophila melanogaster* Schneider's line 2 cells (S2 cells, R690-07, Invitrogen) were cultured in Schneider's medium (Invitrogen) supplemented with 10% fetal calf serum (Thermo) and 1% Penicillin-Streptomycin.

SILAC labelling: S2 cells were cultured in custom-made Schneider's *Drosophila* medium (Athena Enzyme Systems, Baltimore, MD), based on the Invitrogen recipe mentioned above, with several alterations required for the SILAC approach: yeastolate was dialyzed (3500 kD MWCO) and the medium was deficient for both lysine and arginine. Before use, the medium was supplemented with 10% dialyzed Fetal Bovine Serum (F0392, Sigma-Aldrich), 1% Penicillin-Streptomycin and either 2 mg/ml light ($^{12}C6$) lysine (A6969, Sigma-Aldrich) and 0.5 mg/ml light ($^{12}C6$, $^{14}N4$) arginine (L5751, Sigma-Aldrich), or 2 mg/ml heavy ($^{13}C6$) lysine (CLM-2247, Cambridge Isotope laboratories) and 0.5 mg/ml heavy ($^{13}C6$, $^{15}N4$) arginine (CNLM-539, Cambridge Isotope Laboratories). Cells were cultured at 27 °C for at least 7 cell doublings for complete labelling.

dsRNA mediated knockdown: For dsRNA-mediated targeted knockdown studies, S2 cells were treated with dsRNA constructs directed against RPN11 (Uniprot identifier Q9V3H2), USP14 (Q9VKZ8) or UCHL5 (Q9XZ61), or a combination of the latter two, referred in the text to as '2xKD'. Control samples were treated with dsRNA directed against GFP which is not present in the cells used here. The final concentration of total dsRNA was 6μg/ml. In general, S2 cells were incubated with dsRNA at 27°C for 48h (2 days), although some 2xKD experiments were performed for 96h (4 days). dsRNA constructs were synthesized using the Ambion Megascript T7 kit according to the manufacturer's protocol. Oligonucleotide sequences used for dsRNA synthesis can be provided upon request. Knockdown experiments were further performed as described previously (Worby, Simonson-Leff and Dixon, 2001). FACS analysis was performed as described in (Moshkin *et al.*, 2007).

RNA isolation and real time RT-qPCR: For gene expression assays, cell pellets were immediately frozen in liquid nitrogen and stored at -80°C until further processing. Total RNA was extracted from $5x10^6$ cells using Trizol (15596-026, Invitrogen) and 4 μg RNA was used for random hexamer primed cDNA synthesis using the Superscript II Reverse Transcriptase (Invitrogen). Quantitative PCR (qPCR) was performed on a CFX96 realtime PCR detection system (Bio-Rad). Reactions were performed in a total volume of 25 μl containing 1x reaction buffer, SYBR Green I (Sigma), 200 μM dNTPs, 1.5 mM MgCl2, platinum Taq polymerase (Invitrogen), 500 nM of

corresponding primers and 1 µl of cDNA. Primers were made for both the C-terminus and N-terminus of both UCHL5 and USP14. Data analysis was performed by applying the 2-ΔΔCT method (Livak & Schmittgen, 2001). Values obtained from amplification of alpha-1,2-mannosidase (CG11874) were used to normalize the data as described previously (Moshkin *et al.*, 2007).

Antibodies, SDS-PAGE and immunoblotting: Polyclonal antibodies were generated by immunizing guinea pigs or rabbits with GST fusion proteins expressed in *Escherichia coli* and were affinity purified as described previously (Chalkley and Verrijzer, 2004). The following antigens were used: full length Prosalpha5, full length Prosbeta6, full length RPN11, full length RPN8, full length RPN10, full length RPT4 or C-terminal (aa220–405) RPT6. In-house generated polyclonal antibodies used were α-H2B (PV57/58, raised against purified core histones and mainly recognizing H2B, described in (Chalkley and Verrijzer, 2004)) and α-Moira (described in (Mohrmann *et al.*, 2004)). Commercial antibodies against conjugated ubiquitin (FK2, PW8810, Enzo Life Sciences) and Prosalpha subunits (SC-65755, Santa Cruz Biotechnology) were used. SDS-PAGE and immunoblotting experiments were performed as described previously (Chalkley *et al.*, 2008).

Glycerol density gradients: Glycerol gradients were prepared according to (Mohrmann *et al.*, 2004). Briefly, gradients with 5-30% glycerol were prepared in Beckman polyallomer tubes (331374 Beckman). Whole cell lysates were prepared under non-denaturating conditions (50 mM HEPES-KOH pH 7.6, 100 mM KCl, 0.1% NP40, protease inhibitors) and subsequently loaded on top of the gradient and ultracentrifuged (SW40 rotor, Beckman L-80) at 32 krpm for 17 h at 4°C. Twenty-six 500 µl fractions were taken starting from the top of the gradient using a P1000 pipet. Fractions were stored in aliquots at -80°C. Two consecutive fractions were combined starting from fraction 3, resulting in a total of 13 fractions. Of each of these fractions, 25 µl was analyzed by SDS-PAGE and target proteins were visualized by immunoblotting.

Immunopurifications: Immunopurification (IP) procedures were performed essentially as described (Chalkley and Verrijzer, 2004). Briefly, α-RPN8 or α-RPN10 antibodies were crosslinked to Protein A beads by using dimethylpimelimidate. Antibody coupled beads were incubated with whole cell lysate for 2 h. Subsequently, the beads were washed extensively with HEMG based washing buffer containing either 50 mM, 150 mM or 500 mM KCl (25mM HEPES-KOH, pH 7.6, 0.1mM EDTA, 12.5mM MgCl2, 10% glycerol, 50 mM / 150 mM / 500 mM KCl, 0.1% NP-40, containing a standard cocktail of protease inhibitors). Proteins that were retained on the beads were then eluted with 100 mM sodium citrate buffer (pH 2.5), resolved by SDS-PAGE and visualized by Coomassie staining. Finally, lanes were cut in 1 mm slices and prepared for and analyzed by nanoflow LC-MS/MS (see below).

LFQ mass spectrometry: In-gel protein reduction, alkylation and tryptic digestion was performed as described previously (Sap *et al.*, 2015). Peptides were extracted with 30% acetonitrile 0.5% formic

acid and analyzed on an 1100 series capillary LC system (Agilent Technologies) coupled to an LTQ-Orbitrap hybrid mass spectrometer (Thermo). Peptide mixtures were trapped on a ReproSil C18 reversed phase column (Dr Maisch GmbH; column dimensions 2 cm × 100 μm, packed in-house) at a flow rate of 8 μl/min. Peptide separation was performed on a ReproSil C18 reversed phase column (Dr Maisch GmbH; column dimensions 15 cm × 75 μm, packed in-house) using a linear gradient from 0-50% B (A = 0.1% formic acid; B = 80% (v/v) acetonitrile, 0.1% formic acid) in 120 min at a constant flow rate of 300 nl/min using a splitter. The column eluent was directly electrosprayed into the mass spectrometer. Mass spectra were acquired in continuum mode; fragmentation of the peptides was performed in data dependent acquisition mode by CID using top 8 selection.

LFQ data analysis: RAW files were analyzed using MaxQuant software (version 1.5.3.30 | http://www.maxquant.org), which includes the Andromeda search algorithm (Cox *et al.*, 2009, 2011) for searching against the Uniprot database (version January 2016, taxonomy: *Drosophila melanogaster* | http://www.uniprot.org/). Follow-up data analysis was performed using the Perseus analysis framework (http://www.perseus-framework.org/). Perseus (version 1.5.0.31) was used to analyze protein abundance dynamics in the different samples. ProteinGroups.txt files were uploaded to Perseus and rows containing proteins designated 'Only identified by site', 'Reverse' and 'Contaminant' were removed from the matrix. LFQ intensities were Log2-transformed and the LFQ intensity columns of triplicates of RPN8 and RPN10 IPs were grouped together. To ensure a high data quality standard, rows that did not contain at least two valid values in at least one group were removed from the matrix. To identify proteasome interacting proteins, a Welch two-sided t-test was performed for each α-RPN8 or α-RPN10 IP versus the α-PPI (control) IPs. A permutation-based FDR of 0.05 was used for truncation and the number of randomizations was 250. Tables containing proteins with significant abundance changes for each two-sample t-tests were exported to Excel and annotations were added. The software suite R was used to merge the tables for the α-RPN8 or α-RPN10 comparisons with the α-PPI IPs based on the common 'Id' columns. Rows containing significantly changed proteins in the α-RPN8 and α-RPN10 versus control comparisons were merged using R.

Global proteome and diGly-peptide analysis: sample preparation, fractionation & LC-MS/MS: SILAC cell cultures were used for all global proteome and ubiquitinome analyses. After treatment of 2 days (or 4 days) with dsRNA against RPN11, USP14, UCHL5 or GFP (control), cells were harvested and used for 1) immunoblotting or 2) global proteome and ubiquitinome analyses. For immunoblotting, cells were washed 3 times with ice-cold PBS and spun down for 5 min at 1100 rpm at 4°C. Cell pellets were lysed in SDS-PAGE sample buffer (2% SDS, 10% glycerol, 60 mM Tris-HCl pH 6.8, plus protease inhibitors) and lysates were kept on ice and sonicated for 5 min 30 min with an 'on/off' cycle. BCA assay (Pierce) was used to estimate protein concentration. Global proteome and ubiquitinome experiments were performed in duplicate, including a light-heavy label swap ('forward' (light channel DUB treated cells) and 'reverse' (heavy channel DUB

treated cells) experiment). After 2 days (or 4 days) of incubation with dsRNA, cells were harvested, counted (Beckman Coulter Z2) and heavy and light cultures were mixed in a 1:1 ratio (based on cell count). Cells were washed 3 times with ice-cold PBS and lysed in 7 ml lysis buffer (8 M urea, 50 mM Tris-HCl pH 8.0, 50 mM NaCl) for combined global proteome and ubiquitinome analysis. Lysates were incubated on ice for 10 min and sonicated, debris was removed by centrifugation. Protein concentrations were measured in a BCA assay (Pierce). Cell lysates containing 20 mg total protein were collected for combined global proteome and ubiquitinome analyses. Protein lysates were reduced with 10 mM dithiotreitol (DTT) for 1 h at RT followed by alkylation with 55 mM chloroacetamide for 1 h in the dark. The mixture was diluted 1:1 with 50 mM Tris-HCl pH 8.0 and proteins were digested with 1:100 LysC (129-02541 Wako Chemicals) for 1 h at RT. The mixture was diluted with 25 mM Tris HCl (pH 8.2) to a final concentration of 1.6 M urea. $CaCl_2$ was added (1 mM final concentration) and the sample was digested overnight with 1:100 sequencing grade trypsin (cat # 03708969001, Roche) at RT. Peptide mixtures were acidified with 1% trifluoroacetic acid (TFA) and the precipitate was removed by centrifugation. At this point, digests of combined global proteome and ubiquitinome were splitted: 1 mg for the global proteome and approximately 20 mg for the ubiquitinome analysis (same amount of digest for Forward and Reverse). Global proteome digests were desalted using a Sep-Pak® Vac tC18 column (WAT036820, Waters) and eluted with 1 ml 80% acetonitrile / 0.1% FA and fractionated by HILIC on an Agilent 1100 HPLC system using a 5 μm particle size 4.6 x 250 mm TSKgel amide-80 column (Tosoh Biosciences). 200 μg of the desalted tryptic digest in 80% acetonitrile was loaded onto the column. Peptides were eluted using a nonlinear gradient from 80% B (100% acetonitrile) to 100% A (20 mM ammonium formate in water) with a flow of 1 ml/min. Sixteen 6 ml fractions were collected, lyophilized (ScanVac Coolsafe, Scala Scientific) and pooled into 8 final fractions. Each fraction was then analyzed by nanoflow LC-MS/MS as described below.

DiGly-modified peptides were enriched by immunoprecipitation using PTMScan® ubiquitin remnant motif (K-ε-GG) antibody bead conjugate (#5562, Cell Signaling Technology), according to the manufacturer's protocol. Unbound peptides were removed by washing and the captured peptides were eluted with low pH buffer (0.15% TFA). Eluted peptides were analyzed by nanoflow LC-MS/MS.

Nanoflow LC-MS/MS was performed on an EASY-nLC system (Thermo) coupled to a Q Exactive mass spectrometer (Thermo), operating in positive mode and equipped with a nanospray source. Peptide mixtures were trapped on a ReproSil C18 reversed phase column (Dr Maisch GmbH; column dimensions 1.5 cm × 100 μm, packed in-house) at a flow rate of 8 μl/min. Peptide separation was performed on ReproSil C18 reversed phase column (Dr Maisch GmbH; column dimensions 15 cm × 50 μm, packed in-house) using a linear gradient from 0-80% B (A = 0.1% formic acid; B = 80% (v/v) acetonitrile / 0.1% formic acid) in 70 min and at a constant flow rate of 200 nl/min. The column eluent was directly sprayed into the orifice of

the mass spectrometer. Mass spectra were obtained in continuum mode; fragmentation of the peptides was performed in data-dependent mode by HCD using top 15 selection.

SILAC LC-MS/MS data analysis: Mass spectrometric raw data were analyzed using the MaxQuant software (versions 1.5.3.30) for identification and relative quantification of protein groups. A false discovery rate (FDR) of 0.01 for proteins and peptides and a minimum peptide length of 7 amino acids were required. The Andromeda search engine was used to search the MS/MS spectra against the *Drosophila melanogaster* Uniprot database (release 2016_01.fasta, taxonomy: *Drosophila melanogaster*, http://www.uniprot.org/). For SILAC data the multiplicity was set to two and a maximum of two missed cleavages were allowed. The enzyme specificity was set to trypsin and cysteine carbamidomethylation was set as a fixed modification, whereas variable modifications were methionine oxidation, protein N-term acetylation and lysine ubiquitination (GlyGly (K)). The minimum ratio count was set to 1, although peptide spectra for proteins quantified with ratio count 1 were checked manually for data quality. Only proteins that were identified and quantified in both forward and reverse experiments and with consistent ratios, were taken into account for further analysis. Protein sets were further functionally analyzed using Perseus (version 1.5.0.31), the gene ontology (GO) software DAVID (version 6.7, available from http://david.abcc.ncifcrf.gov/) and in-house developed software.

References

Aufderheide, A. *et al.* (2015) 'Structural characterization of the interaction of Ubp6 with the 26S proteasome.', *Proceedings of the National Academy of Sciences of the United States of America*, 112(28), pp. 8626–31.

Bashore, C. *et al.* (2015) 'Ubp6 deubiquitinase controls conformational dynamics and substrate degradation of the 26S proteasome', *Nature Structural & Molecular Biology*. Nature Publishing Group, 22(9), pp. 712–719.

Borodovsky, A. *et al.* (2001) 'A novel active site-directed probe specific for deubiquitylating enzymes reveals proteasome association of USP14', *EMBO Journal*, 20(18), pp. 5187–5196.

Brnjic, S. *et al.* (2013) 'Induction of Tumor Cell Apoptosis by a Proteasome Deubiquitinase Inhibitor Is Associated with Oxidative Stress.', *Antioxidants & redox signaling*, 21(17), p. 24011031.

Chalkley, G. E. *et al.* (2008) 'The transcriptional coactivator SAYP is a trithorax group signature subunit of the PBAP chromatin remodeling complex.', *Molecular and cellular biology*, 28(9), pp. 2920–9.

Chalkley, G. E. and Verrijzer, C. P. (2004) 'Immuno-Depletion and Purification Strategies to Study Chromatin-Remodeling Factors In Vitro', *Methods in Enzymology*, 377(2001), pp. 421–442.

Chen, X. *et al.* (2010) 'Structure of proteasome ubiquitin receptor hRpn13 and its activation by the scaffolding protein hRpn2.', *Molecular cell*. United States, 38(3), pp. 404–415.

Chernova, T. A. *et al.* (2003) 'Pleiotropic Effects of Ubp6 Loss on Drug Sensitivities and Yeast Prion Are Due to Depletion of the Free Ubiquitin Pool', *Journal of Biological Chemistry*. in Press, 278(52), pp. 52102–52115.

Cox, J. *et al.* (2009) 'A practical guide to the MaxQuant computational platform for SILAC-

based quantitative proteomics.', *Nature protocols*, 4, pp. 698–705.

Cox, J. *et al.* (2011) 'Andromeda: a peptide search engine integrated into the MaxQuant environment.', *Journal of proteome research*, 10(4), pp. 1794–805.

D'Arcy, P. *et al.* (2011) 'Inhibition of proteasome deubiquitinating activity as a new cancer therapy', *Nature Medicine*, 17(12), pp. 1636–1641.

Elena Koulich, Xiaohua Li, and G. N. D. (2008) 'Relative Structural and Functional Roles of Multiple Deubiquitylating Proteins Associated with Mammalian 26S Proteasome', *Molecular biology of the cell*, 19, pp. 1072–1082.

Elsasser, S. *et al.* (2002) 'Proteasome subunit Rpn1 binds ubiquitin-like protein domains', *Nature Cell Biology*, 4(9), pp. 725–730.

Feng, X. *et al.* (2014) 'Proapoptotic effects of the novel proteasome inhibitor b-AP15 on multiple myeloma cells and natural killer cells', *Experimental Hematology*. ISEH - Society for Hematology and Stem Cells, 42(3), pp. 172–182.

Finley, D. *et al.* (1998) 'Unified nomenclature for subunits of the Saccharomyces cerevisiae proteasome regulatory particle.', *Trends in biochemical sciences*. ENGLAND, pp. 244–245.

Finley, D. (2009) 'Recognition and Processing of Ubiquitin-Protein Conjugates by the Proteasome', *Annual review of biochemistry,* pp. 477–513

Flierman, D. *et al.* (2016) 'Non-hydrolyzable Diubiquitin Probes Reveal Linkage-Specific Reactivity of Deubiquitylating Enzymes Mediated by S2 Pockets', *Cell Chemical Biology*, 23(4), pp. 472–482.

Fu, H. *et al.* (2002) 'Subunit interaction maps for the regulatory particle of the 26S proteasome and the COP9 signalosome', *EMBO Journal*, 20(24), pp. 7096–7107.

Gallery, M. *et al.* (2007) 'The JAMM motif of human deubiquitinase Poh1 is essential for cell viability', *Molecular Cancer Therapeutics*, 6(1), pp. 262–268.

Guterman, A. and Glickman, M. H. (2004) 'Complementary Roles for Rpn11 and Ubp6 in Deubiquitination and Proteolysis by the Proteasome', *Journal of Biological Chemistry*, 279(3), pp. 1729–1738.

Hamazaki, J. *et al.* (2006) 'A novel proteasome interacting protein recruits the deubiquitinating enzyme UCH37 to 26S proteasomes', *The EMBO Journal*, 25(19), pp. 4524–4536.

Hanna, J. *et al.* (2006) 'Deubiquitinating Enzyme Ubp6 Functions Noncatalytically to Delay Proteasomal Degradation', *Cell*, 127(1), pp. 99–111.

Hanna, J., Leggett, D. S. and Finley, D. (2003) 'Ubiquitin depletion as a key mediator of toxicity by translational inhibitors', *Molecular and Cellular Biology*, 23(24), pp. 9251–9261.

Hochstrasser, R. J. T. J. and M. (2013) 'Molecular Architecture and Assembly of the Eukaryotic proteasome', (3).

Hölzl, H. *et al.* (2000) 'The regulatory complex of Drosophila melanogaster 26S proteasomes. Subunit composition and localization of a deubiquitylating enzyme.', *The Journal of cell biology*, 150(1), pp. 119–30.

Hu, M. *et al.* (2005) 'Structure and mechanisms of the proteasome-associated deubiquitinating enzyme USP14', *The EMBO Journal*, 24(21), pp. 3747–3756.

Huang, L., Jung, K. and Chen, C. H. o (2014) 'Inhibitory effect of b-AP15 on the 20S proteasome', *Biomolecules*, 4(4), pp. 931–939.

Kaiser, S. E. *et al.* (2011) 'Protein standard absolute quantification (PSAQ) method for the measurement of cellular ubiquitin pools.', *Nature methods*, 8(8), pp. 691–6.

Kim, H. T. and Goldberg, A. L. (2017) 'The Deubiquitinating Enzyme Usp14 Allosterically Inhibits Multiple Proteasomal Activities and Ubiquitin-Independent Proteolysis.', *The Journal of biological chemistry*, (3), p. jbc.M116.763128.

Komander, D., Clague, M. J. and Urbe, S. (2009) 'Breaking the chains: structure and function of the deubiquitinases', *Nat Rev Mol Cell Biol*. Nature Publishing Group, 10(8), pp. 550–563.

Kuo, C.-L. and Goldberg, A. L. (2017) 'Ubiquitinated proteins promote the association of proteasomes with the deubiquitinating enzyme Usp14 and the ubiquitin ligase Ube3c', *Proceedings of the National Academy of Sciences*, 114(17), pp. E3404–E3413.

Lam, Y. A. *et al.* (1997) 'Editing of ubiquitin conjugates by an isopeptidase in the 26S proteasome.', *Nature*, pp. 737–740.

Lee, B.-H. *et al.* (2010) 'Enhancement of proteasome activity by a small-molecule inhibitor of USP14', *Nature*. Nature Publishing Group, 467(7312), pp. 179–184.

Lee, B.-H. *et al.* (2016) 'USP14 deubiquitinates proteasome-bound substrates that are ubiquitinated at multiple sites', *Nature*. Nature Publishing Group, pp. 1–16.

Lee, M. J. *et al.* (2011) 'Trimming of ubiquitin chains by proteasome-associated deubiquitinating enzymes.', *Molecular & cellular proteomics : MCP*, 10(5), p. R110.003871.

Leggett, D. S. *et al.* (2002) 'Multiple associated proteins regulate proteasome structure and function', *Molecular Cell*, 10(3), pp. 495–507.

Li, T. T. *et al.* (2000) 'Identification of a 26S proteasome-associated UCH in fission yeast.', *Biochemical and biophysical research communications*, 272(1), pp. 270–275.

Livak, K. J., & Schmittgen, T. D. (2001). Analysis of relative gene expression data using real-time quantitative PCR and the 2(-Delta Delta C(T)) Method. *Methods* (San Diego, Calif.), 25(4), 402–408.

Lundgren, J. *et al.* (2003) 'Use of RNA Interference and Complementation To Study the Function of the Drosophila and Human 26S Proteasome Subunit S13', *Mol Cell Biol*, 23(15), pp. 5320–5330.

Mansour, W. *et al.* (2015) 'Disassembly of Lys<inf>11</inf> and mixed linkage polyubiquitin conjugates provides insights into function of proteasomal deubiquitinases Rpn11 and Ubp6', *Journal of Biological Chemistry*, 290(8), pp. 4688–4704.

Matiuhin, Y. *et al.* (2008) 'Extraproteasomal Rpn10 Restricts Access of the Polyubiquitin-Binding Protein Dsk2 to Proteasome', *Molecular Cell*. Elsevier Inc., 32(3), pp. 415–425.

Matyskiela, M. E., Lander, G. C. and Martin, A. (2013a) 'Conformational switching of the 26S proteasome enables substrate degradation.', *Nature structural & molecular biology*. 20(7), pp. 781–8.

Maytal-Kivity, V. *et al.* (2002) 'MPN+, a putative catalytic motif found in a subset of MPN domain proteins from eukaryotes and prokaryotes, is critical for Rpn11 function.', *BMC biochemistry*, 3, p. 28.

Mazumdar, T. *et al.* (2010) 'Regulation of NF-kappaB activity and inducible nitric oxide synthase by regulatory particle non-ATPase subunit 13 (Rpn13).', *Proceedings of the National Academy of Sciences of the United States of America*, 107(31), pp. 13854–13859.

Mialki, R. K. *et al.* (2013) 'Overexpression of USP14 protease reduces I-??B protein levels and increases cytokine release in lung epithelial cells', *Journal of Biological Chemistry*, 288(22), pp. 15437–15441.

Mohrmann, L. *et al.* (2004) 'Differential Targeting of Two Distinct SWI / SNF-Related Drosophila Chromatin-Remodeling Complexes Differential Targeting of Two Distinct SWI / SNF-Related Drosophila Chromatin-Remodeling Complexes', 24(8), pp. 3077–3088.

Moshkin, Y. M. *et al.* (2007) 'Functional differentiation of SWI/SNF remodelers in transcription and cell cycle control.', *Molecular and cellular biology*, 27, pp. 651–661.

Ortuno, D., Carlisle, H. J. and Miller, S. (2016) 'Does inactivation of USP14 enhance degradation of proteasomal substrates that are associated with neurodegenerative diseases ? *F1000Research* 5(137)

Pathare, G. R. *et al.* (2014) 'Crystal structure of the proteasomal deubiquitylation module Rpn8-Rpn11', *Proceedings of the National Academy of Sciences*, 111(8), pp. 2984–2989.

Peth, A., Besche, H. C. and Goldberg, A. L. (2009) 'Ubiquitinated Proteins Activate the Proteasome

by Binding to Usp14/Ubp6, which Causes 20S Gate Opening', *Molecular Cell*, 36(5), pp. 794–804.

Qiu, X. *et al.* (2006) 'hRpn13/ADRM1/GP110 is a novel proteasome subunit that binds the deubiquitinating enzyme, UCH37', *The EMBO Journal*, 25(24), pp. 5742–5753.

Rosenzweig, R. *et al.* (2012) 'Rpn1 and Rpn2 coordinate ubiquitin processing factors at proteasome', *Journal of Biological Chemistry*, 287(18), pp. 14659–14671.

Sanches, M. *et al.* (2007) 'The Crystal Structure of the Human Mov34 MPN Domain Reveals a Metal-free Dimer', *Journal of Molecular Biology*, 370(5), pp. 846–855.

Sap, K. A. *et al.* (2015) 'Global quantitative proteomics reveals novel factors in the ecdysone signaling pathway in Drosophila melanogaster', *Proteomics*, 15(4), pp. 725–738.

Sap, K. A. *et al.* (2017) 'Quantitative Proteomics Reveals Extensive Changes in the Ubiquitinome after Perturbation of the Proteasome by Targeted dsRNA-Mediated Subunit Knockdown in Drosophila', *Journal of Proteome Research*, 16(8), pp. 2848–2862.

Tian, Z. *et al.* (2014) 'A novel small molecule inhibitor of deubiquitylating enzyme USP14 and UCHL5 induces apoptosis in multiple myeloma and overcomes bortezomib resistance', *Blood*, 123(5), pp. 706–716.

Udeshi, N. D. *et al.* (2012) 'Methods for Quantification of in vivo Changes in Protein Ubiquitination following Proteasome and Deubiquitinase Inhibition', *Molecular & Cellular Proteomics*, 11, pp. 148–159.

Unverdorben, P. *et al.* (2014) 'Deep classification of a large cryo-EM dataset defines the conformational landscape of the 26S proteasome.', *Proceedings of the National Academy of Sciences of the United States of America*, 111(15), pp. 5544–9.

Verma, R. *et al.* (2002) 'Role of Rpn11 Metalloprotease in Deubiquitination and Degradation by the 26S Proteasome', *Science*, 298(5593), pp. 611–615.

Wagner, S. a *et al.* (2011) 'A Proteome-wide, Quantitative Survey of In Vivo Ubiquitylation Sites Reveals Widespread Regulatory Roles.', *Molecular & cellular proteomics : MCP*, 10(10), p. M111.013284.

Van Der Wal, L. *et al.* (2018) 'Improvement of ubiquitylation site detection by Orbitrap mass spectrometry', *Journal of Proteomics*, 172, pp. 49–56.

Wang, X. *et al.* (2014) 'The 19S Deubiquitinase inhibitor b-AP15 is enriched in cells and elicits rapid commitment to cell death.', *Molecular pharmacology*, 85(6), pp. 932–45.

Wójcik, C. and DeMartino, G. N. (2002) 'Analysis of Drosophila 26 S proteasome using RNA interference.', *The Journal of biological chemistry*, 277(8), pp. 6188–97.

Worby, C. A., Simonson-Leff, N. and Dixon, J. E. (2001) 'RNA interference of gene expression (RNAi) in cultured Drosophila cells.', *Science's STKE : signal transduction knowledge environment*. United States, 2001(95), p. pl1.

Worden, E. J., Dong, K. C. and Martin, A. (2017) 'An AAA Motor-Driven Mechanical Switch in Rpn11 Controls Deubiquitination at the 26S Proteasome', *Molecular Cell*. Elsevier Inc., pp. 1–13.

Worden, E. J., Padovani, C. and Martin, A. (2014a) 'Structure of the Rpn11-Rpn8 dimer reveals mechanisms of substrate deubiquitination during proteasomal degradation.', *Nature structural & molecular biology*. Nature Publishing Group, 21(3), pp. 220–7.

Yao, T. *et al.* (2006) 'Proteasome recruitment and activation of the Uch37 deubiquitinating enzyme by Adrm1', *Nature Cell Biology*, 8(9), pp. 994–1002.

Yao, T. and Cohen, R. E. (2002) 'A cryptic protease couples deubiquitination and degradation by the proteasome.', *Nature*, 419(6905), pp. 403–407.

Supporting information available online

Table 1 | Numbers of identified and quantified proteins in the global proteome datasets

Table 2 | Numbers of identified and quantified diGly modified peptides

(The 3xKD dataset published previously (Sap *et al.*, 2017) serve as a reference.)

Supporting information available in this thesis

Supplementary Table S1 |List of proteins with decreased abundances upon RPN11 KD

Supplementary Table S2 | List of proteins with increased abundances upon USP14 KD, UCHL5 and 2xKD

Supplementary Table S3 | List of proteins with decreased abundance upon USP14 KD, UCHL5 and 2xKD

Supplementary Table S4 | List of diGly modified peptides with decreased abundances upon RPN11 KD

Supplementary Table S5 | List of diGly modified peptides with increased abundances upon USP14 KD, UCHL5 or 2xKD

Supplementary Table S6 | List of diGly modified peptides with decreased abundances upon USP14 KD, UCHL5 or 2xKD

Table S1. List of proteins with decreased abundance upon Rpn11 KD

Protein names	Gene names	Down Rpn11 KD	Down 2d 3xKD	Description
Organic cation transporter-like protein	Orct2	+	+	Positive regulation of cell growth, organic cation transport
Intronic protein 259	Ip259	+	+	Phagocytosis, neurogenesis
CG4829	CG4829	+	+	Glutathione metabolic process, neuron projection morphogenesis
26S proteasome non-ATPase regulatory subunit 14	Rpn11	+	+	Proteasome DUB
CG8034	CG8034	+	+	Transmembrane transport
Parathion hydrolase-related protein	CG18473	+	+	Hydrolase, catabolic process
Glutathione S transferase T4	GstT4	+	+	Glutathione transferase activity
CG13367	CG13367	+		Unknown
CG32850	CG32850	+		Ubiquitin ligase, structurally related to RNF11
Coenzyme Q-binding protein COQ10, mitochondrial	Coq10	+		Mitochondrial membrane protein, required for the function of coenzyme Q in the respiratory chain
Transmembrane protein windpipe	wdp	+		Trachea development, synaptic target recognition
Viking	vkg	+		Extracellular matrix structural constituent
Division abnormally delayed	dally	+		Cell surface proteoglycan that bears heparan sulfate
CG6860	Lrch	+		Cell cortex, Ras protein signal transduction
Fat-spondin	fat-spondin	+		Extracellular region, serine-type endopeptidase inhibitor activity
CG10184	CG10184	+		Cellular amino acid metabolic process
Tiggrin	Tig	+		Cell adhesion, phagocytosis, axon guidance
CG15820	CG15820	+		Unknown
Phosphoenolpyruvate carboxykinase	Pepck ZDF4	+		Carbohydrate biosynthesis
CG18088	CG18088	+		Metabolic process
CG13366	CG13366	+		Developmental protein
CG33462	CG33462	+		Proteolysis, serine-type endopeptidase activity

Table S2. Proteins with increased abundance upon UCHL5 KD, USP14 KD or 2xKD

Protein names	Gene names	Up UchL5 KD	Up USP14 KD	Up 2d 2xKD	Up 4d 2xKD	Up 2d 3xKD	Up Rpn11 KD	Description
CG7222	CG7222	+				+	+	Unknown
Puckered	puc	+				+		JUN kinase phosphatase
Attacin-D	AttD	+				+		Defense response to Gram-positive bacteria
CG7130	CG7130	+				+		Unknown
Glutathione S transferase S1	GstS1	+						Glutathione peroxidase activity
Glutathione S-transferase D2	GstD2	+						Glutathione peroxidase activity
CG6674	CG6674	+						Unknown
Drosha	drosha	+						Primary miRNA processing
Vacuolar H[+] ATPase M9.7 subunit c	VhaM9.7-c	+						ATP hydrolysis coupled proton transport
Real-time	retm		+					phosphatidylinositol transporter activity
CG32039	CG32039		+					Unknown
CG7200	CG7200		+					Unknown
CG31886	CG31886			+				Unknown
TMS1	TMS1			+				Unknown
cAMP-dependent protein kinase type II regulatory subunit	Pka-R2			+				cAMP-binding, axon guidance
CG6650	CG6650			+				Carbohydrate metabolic process
CG9691	CG9691			+				Unknown
Tubulin gamma chain	gammaTub37C				+	+		Major constituent of microtubules
Histone H3-like centromeric protein cid	cid				+			Histone H3-like variant required for recruitment and assembly of kinetochore proteins, mitotic progression and chromosome segregation
CG33096	CG33096				+			Hydrolase
Fu2	fu2				+			Nucleic acid binding
CG4901	CG4901				+			ATP-dependent RNA helicase activity
tamas	tam				+			Replication of mitochondrial DNA
CG16771	CG16771				+			Alkaline phosphatase activity
Methyltransferase-like protein 14 homolog	CG7818				+			mRNA methylation
Mutator 2	mu2				+			Double-strand break repair

Table S3. List of proteins with decreased abundance upon UCHL5 KD, USP14 KD or 2xKD

Protein names	Gene names	Down UchL5 KD	Down USP14 KD	Down 2d 2xKD	Down 4d 2xKD	Down Rpn11 KD	Down 2d 3xKD	Description
Ubiquitin carboxyl-terminal hydrolase	UCHL5	+		+	+			Proteasome DUB
Protein cueball	cue	+					+	Wnt-activated receptor activity
KLHL18	KLHL18	+						Actin-binding
Kokopelli	koko	+						Regulation of cyclin-dependent protein serine/threonine kinase activity
CG42307	mus312	+						Unknown
Anaphase-promoting complex subunit 10	APC10	+						Component of the Anaphase-promoting complex, cell cycle regulation
Probable cytochrome P450 12a5, mitochondrial	Cyp12a5	+						Oxidoreductase
Ubiquitin carboxyl-terminal hydrolase	USP14		+	+	+			Proteasome DUB
CG9691	CG9691		+					Unknown
Kinetochore protein Spc25	Spc25		+					Component of Ndc80 complex, chromosome segregation, spindle checkpoint, kinetochore integrity, organization of stable microtubule binding sites
Expanded	ex		+					Endocytic recycling, negative regulation of proliferation and growth
DREV1	Rev1 drev1		+					Regulation of double-strand break repair via homologous recombination
Protein gustavus	gus		+					Developmental protein, primordial germ cell formation
Beta-glucuronidase	CG15117		+					Lysosome, degradation of dermatan and keratan sulfates
Nuclear export factor 3	Nxf3		+					mRNA export from nucleus
CG8170	CG8170		+					Proteolysis, serine-type endopeptidase activity
Saxophone	sax		+					Kinase, developmental protein, actin filament organization
Mei-P26	mei-P26		+					Ubiquitin ligase, meiotic nuclear division
CG30116	CG30116		+					Peptidase activator activity involved in apoptotic process
CG10188	CG10188		+					Positive regulation of Rho protein signal transduction
CG30387	CG30387		+					Unknown
Ankyrin 2	Ank2		+					Cytoskeleton protein binding, signal transduction
CG9780	CG9780		+					Proteolysis, metalloendopeptidase activity
CG3563	jvl		+					Developmental protein, actin filament bundle assembly
Glycerol kinase	Gk		+					Carbohydrate metabolic process
Insulin-like receptor	InR dinr Dir-a Inr-a		+					Ligand-stimulated tyrosine-protein kinase activity. Regulates body size and organ size, involved in development of embryonic nervous system.
LpR2	LpR2		+					Neuron projection morphogenesis
CG13001	CG13001			+				Unknown
CG2698	CG2698			+				Unknown
Serine protease 7 3.4.21.	Sp7			+				Proteolysis, carboxypeptidase activity
Cyclin A	CycA				+			Regulation of cyclin-dependent protein serine/threonine kinase activity
Cappuccino	capu				+			Actin nucleation
CG30359	Mal-A5				+			Carbohydrate metabolic process
CG41434	CG41434				+			Unknown
RabX4	RabX4				+			Protein transport, recycling endosome
CG10903	CG10903				+			Neurogenesis, methyltransferase activity

Table S4. Selection of proteins with increased abundance upon both 3xKD & Rpn11 KD

Entry	Protein names	Gene names	protein catabolic process	proteolysis	Cytoskeleton organization	Description
P40301	Proteasome subunit alpha type-2	Prosalpha2	protein catabolic process	proteolysis	cytoskeleton organization	20S Proteasome subunit alpha
P18053	Proteasome subunit alpha type-4	Prosalpha3	protein catabolic process	proteolysis	cytoskeleton organization	20S Proteasome subunit alpha
P22769	Proteasome subunit alpha type-7-1	Prosalpha4	protein catabolic process	proteolysis		20S Proteasome subunit alpha
A0AQH0	Proteasome subunit beta type	Prosbeta1	protein catabolic process	proteolysis		20S Proteasome catalytic subunit
Q9VUJ1	Proteasome subunit beta type	Prosbeta2	protein catabolic process	proteolysis		20S Proteasome catalytic subunit
Q9XYN7	Proteasome subunit beta type-3	Prosbeta3	protein catabolic process	proteolysis		20S Proteasome subunit beta
Q9VJJ0	Proteasome subunit beta type	Prosbeta4	protein catabolic process	proteolysis		20S Proteasome subunit beta
Q7KMQ0	Rpt1	Rpt1	protein catabolic process			20S Regulatory particle triple A
P48601	26S protease regulatory subunit 4	Rpt2	protein catabolic process	proteolysis	cytoskeleton organization	20S Regulatory particle triple A
Q9W414	Regulatory particle triple-A ATPase 4	Rpt4	protein catabolic process			20S Regulatory particle triple A
Q9V3V6	26S proteasome regulatory complex subunit p50	Rpt5	protein catabolic process			20S Regulatory particle triple A
Q9VW54	26S proteasome regulatory complex subunit p97	Rpn1			cytoskeleton organization	Proteasome regulatory subunit
Q9VKZ8	USP14	USP14	protein catabolic process	proteolysis		DUB proteasome
Q9VH79	Rpt3R	Rpt3R	protein catabolic process			ATP binding
Q9VA54	Rpt6R	Rpt6R	protein catabolic process			ATP binding
Q9VN58	CG42574	ctrip	protein catabolic process	proteolysis		Ubiquitin ligase, circadian rhythm
Q7YZ96	CG9772	Skp2	protein catabolic process	proteolysis		SCF ubiquitin ligase complex
A1Z7K9	CG8232	PAN2	protein catabolic process	proteolysis		poly(A) specific ribonuclease activity
Q24044	Fizzy	fzy	protein catabolic process	proteolysis		Anaphase Promoting Complex
Q7KN62	Transitional endoplasmic reticulum ATPase TER94	TER94	protein catabolic process	proteolysis	cytoskeleton organization	ER and Golgi vesicle transport, UPS, oskar mRNA localization
Q7JQI1	CG8830	DUBAI	protein catabolic process			Deubiquitinating apoptotic inhibitor
Q9VM45	Nuf2	Nuf2			cytoskeleton organization	Ndc80 complex, kinetochore
Q9VRK9	Kinesin-like protein at 64D	Klp64D			cytoskeleton organization	kinesin complex
Q9VKN7	Aurora kinase B	ial			cytoskeleton organization	Regulates chromosome segregation
Q8SX98	Verprolin 1	Vrp1			cytoskeleton organization	Actin filament organization
Q8SXX1	Phosphatidylinositol 5-phosphate 4-kinase	PIP4K			cytoskeleton organization	Actin filament organization
P35220	Catenin alpha	alpha-Cat			cytoskeleton organization	Interaction with cadherins, cell adhesion
Q9VIJ5	Pomp	Pomp			cytoskeleton organization	mitotic spindle elongation, proteasome maturation protein
A4V164	Phosphoinositide-dependent kinase 1	Pdk1			cytoskeleton organization	required for actin cytoskeleton stability
P20439	G2/mitotic-specific cyclin-B	CycB			cytoskeleton organization	Essential for the control of the cell cycle at the G2/M (mitosis) transition
Q9V9Y9	Spn-F	spn-F			cytoskeleton organization	minus-end-directed microtubule motor activity
Q9VGF9	Aurora	aur			cytoskeleton organization	Kinase, centrosome separation
Q9VSW5	Kinesin-like protein at 67A	Klp67A			cytoskeleton organization	Plus-end-directed microtubule motor activity
Q9VNS0	Protein maelstrom	mael			cytoskeleton organization	Position microtubule-organizing center in oocytes
Q9V3V7	Kinetochore protein Spc25	Spc25			cytoskeleton organization	Ndc80 complex, kinetochore integrity
Q59DY7	Grapes	grp			cytoskeleton organization	Centrosome separation, mitotic cell cycle checkpoint
Q6NN29	Nuclear fallout	nuf			cytoskeleton organization	Actin cytoskeleton reorganization

Table S5. List of diGly peptides with decreased abundance upon Rpn11 KD

Gene names	Protein names	Description	Sequence	Down Rpn11 KD	Down 2d 3xKD
RpS2 sop	40S ribosomal protein S2 (Protein strings of pearls)	Protein synthesis, developmental protein	EMPLGSTPYQAYSDFLSKPTPR	+	+
			EMPLGSTPYQAYSDFLSKPTPR	+	+
			EDSKEWVPVTK	+	
RpS3	40S ribosomal protein S3	Cytoplasmic translation, DNA repair	KPLPDNVSVVEPKEEK	+	+
RpL11	60S ribosomal protein L11	Structural constituent of ribosome, rRNA binding, mitotic spindle organization, centrosome duplication	VLEQLTGQQPVFSKAR	+	
RpL22	60S ribosomal protein L22	Structural constituent of ribosome, mitotic spindle elongation, translation	VNGKVNNLGNNVTFER	+	
			VVANEKDSYELR	+	
path	Pathetic	Amino acid transmembrane transporter activity, growth	VMYKIQPR	+	
			HAPQEMEQFLPGEGKVMYK	+	
CG8177	CG8177	Membrane protein, inorganic anion exchanger	YNSYTSLQNLSGTDDKK	+	+
Orct2	Organic cation transporter-like protein	Organic cation transmembrane transporter activity, positive regulation of cell growth	APEAQPLKGSGETNGSTIANGHK	+	+
			GSGETNGSTIANGHK	+	
Vha55	V-type proton ATPase subunit B	ATP hydrolysis coupled proton transport, vacuolar acidification	FPKFAEIVQLR	+	
Gp150	Gp150 protein	Transmembrane receptor protein tyrosine phosphatase signaling pathway	LSEDIVKPTSKEQK	+	
			LSEDIVKPTSK	+	
			NSFVYQKLSEDIVKPTSK	+	
			MALLASKNSFVYQK	+	+
CG8468	CG8468	Transmembrane transport	GLVSKQPENIK	+	
			SQDELASKGLVSK	+	+
ClC-b	CG8594	Ion transport, sensory perception of touch	EAGPTSKAVQDFGLHQR	+	
CG5021	Uncharacterized Golgi apparatus membrane protein-like protein CG5021	Multipass membrane protein	DLNSAATDFVKTQFFK	+	
Sdc Syd	Syndecan	Cell surface proteoglycan, energy homeostasis, axon guidance	RSPANNSYAKNANNR	+	
wgn	TNFR superfamily protein Wengen)	Tumor necrosis factor-activated receptor activity, apoptotic process, cell surface receptor signaling pathway	RLDQDVEELSTKLMAK	+	
egh zw4	Protein egghead	Axon guidance, cell fate commitment, developmental protein	FYVVQKDVR	+	
CG3164	CG3164	Hydrolase, ATPase activity	LGTAGAGQLKAQIVPAQPK	+	+
			TKNDNANLLNDNR	+	+
			ARNDLVKVQNLK	+	+
			NDLVKVQNLK	+	+
			AQIVPAQPKTLQHLPK	+	+
CG16771	CG16771	Alkaline phosphatase activity, metabolic process	RSGTPINSQKFR	+	
rost	Protein rolling stone	Developmental protein, muscle protein, myoblast fusion	MQLFDDFCKSFNK	+	+
			MQLFDDFCKSFNK	+	
CG4668	CG42389	Unknown	GPETKFTIDNLAAGTCYQFR	+	+
			IVCKVTSLYSNR	+	

Table S6.List of diGly peptides with increased abundance upon UCHL5 KD, USP14 KD or 2xKD

Gene Names	Protein Names	Description	Sequence	UchL5 KD	USP14 KD	2d 2xKD	4d2xKD	2d 3xKD	Rpn11 KD
ref(2)P	Protein ref(2)P	Clearance protein aggregates	CELAHKHPEHLMLR	+					+
CaBP1	Calcium-binding protein 1	Protein disulfide isomerase activity, protein folding, cell redox homeostasis	GFPTIKIFGANK	+					
pirk	Poor Imd response upon knock-in	Negative regulation of immune response	NAKPTPTDAGQGK	+					
LanB2	Laminin subunit gamma-1	cell adhesion	ALADKLESEAQFDLK		+			+	
Mct1	Monocarboxylate transporter 1	transmembrane transport	VLPKDQYLQLPQRTDTAVSGGALCR		+				
key	NF-kappa-B essential modulator	Positive regulation immune response	QEVIKGLQIQNDIYR			+		+	+
RpS11	40S ribosomal protein S11	rRNA binding, translation, mitotic spindle	AFQKQFGVNLNRK			+			
CG5555	CG5555	Zinc ion binding	LFQNKSDGKLVASQTEK				+	+	+
			SDGKLVASQTEKDEREEK				+	+	+
Rpt3;Rpt3R	26S proteasome regulatory complex subunit p48A	Proteasome subunit	VVGSEFVQKYLGEGPR				+	+	+
CG9372	CG9372	serine-type endopeptidase activity	MPELKNDVWR				+	+	+
blanks	blanks	RNA interference, regulation of chromatin silencing	MEAKQLLAESCAK				+	+	
CG5555	CG5555	Zinc ion binding	SDGKLVASQTEKDER				+		+
RpL15	60S ribosomal protein L15	Structural constituent of the ribosome, translation	AKQGFVIYR				+		+
Argk	Arginine kinase	phosphorylation	AVQQQLIDDHFLFKEGDRFLQAANACR				+		
eca;p24-2	Transmembrane emp24 domain-containing protein eca	Developmental protein, Wnt signaling, ER to Golgi-vesicle mediated transport	QLLDQVEQITKEQNYQR				+		
CG2765	CG2765	myosin binding	SGYTDLTKLETSR				+		
CG18343-RA	CG18343	Unknown	MEKSCSIGNGR				+		
RpL13	60S ribosomal protein L13	Structural constituent of the ribosome, translation, mitotic spindle	GPVLPIKNEQPAVVEFR				+		